Universität des Saarlandes

Fachrichtung 6.1 – Mathematik

Preprint Nr. 331

Interface dynamics in discrete forward-backward diffusion equations

Michael Helmers and Michael Herrmann

Saarbrücken 2013

Fachrichtung 6.1 – Mathematik
Universität des Saarlandes

Preprint No. 331
submitted: April 5, 2013

Interface dynamics in discrete forward-backward diffusion equations

Michael Helmers

Universität Bonn
Institut für Angewandte Mathematik
Endenicher Allee 60
D-53115 Bonn
Germany
helmers@iam.uni-bonn.de

Michael Herrmann

Universität des Saarlandes
Fachrichtung Mathematik
Postfach 151150
D-66041 Saarbrücken
Germany
michael.herrmann@math.uni-sb.de

Edited by
FR 6.1 – Mathematik
Universität des Saarlandes
Postfach 15 11 50
66041 Saarbrücken
Germany

Fax: + 49 681 302 4443
e-Mail: preprint@math.uni-sb.de
WWW: http://www.math.uni-sb.de/

Interface dynamics in discrete forward-backward diffusion equations

Michael Helmers* Michael Herrmann†

April 5, 2013

Abstract

We study the motion of phase interfaces in a diffusive lattice equation with bistable nonlinearity and derive a free boundary problem with hysteresis to describe the macroscopic evolution in the parabolic scaling limit.

The first part of the paper deals with general bistable nonlinearities and is restricted to numerical experiments and heuristic arguments. We discuss the formation of macroscopic data and present numerical evidence for pinning, depinning, and annihilation of interfaces. Afterwards we identify a generalized Stefan condition along with a hysteretic flow rule that characterize the dynamics of both standing and moving interfaces.

In the second part, we rigorously justify the limit dynamics for single-interface data and a special piecewise affine nonlinearity. We prove persistence of such data, derive upper bounds for the macroscopic interface speed, and show that the macroscopic limit can indeed be described by the free boundary problem. The fundamental ingredient to our proofs is a representation formula that links the solutions of the nonlinear lattice to the discrete heat kernel and enables us to derive macroscopic compactness results in the space of continuous functions.

Keywords: *forward-backward diffusion in lattices, coarse graining for gradient flows, hysteretic models for phase transitions, pinning and depinning of interfaces, regularization of ill-posed parabolic PDEs*

MSC (2010): 34A33, 35R25, 37L60, 74N20, 74N30

Contents

*helmers@iam.uni-bonn.de, Institut für Angewandte Mathematik, Universität Bonn.

†michael.herrmann@math.uni-sb.de, Fachrichtung Mathematik, Universität des Saarlandes.

1 Introduction

Discrete forward-backward diffusion equations appear in many different applications such as edge-detection in digital images [PM90], models for population dynamics based upon random walks on lattices [HPO04], or phase transition problems with supercooling and superheating [Ell85]. In all applications it is a common major problem to understand how the backward-parabolic regions affect the dynamics on large scales. In this paper, we study the diffusion lattice

$$\dot{u}_j(t) = \Delta\, \Phi'(u_j(t)) \tag{1.1}$$

for $j \in \mathbb{Z}$, $t \geq 0$, or equivalently

$$\dot{w}_j(t) = \nabla_- \Phi'(\nabla_+ w_j(t)). \tag{1.2}$$

Here ∇_-, ∇_+ are the left- and right-sided discrete difference operators, Δ denotes the standard discrete Laplacian $\Delta\, p_j = p_{j+1} - 2p_j + p_{j-1}$, and u_j, w_j are connected via $u_j = \nabla_+ w_j$. As illustrated in Figure 1.1, we always suppose that Φ' the derivative of a double-well potential Φ, so it consists of two stable branches that enclose an unstable one.

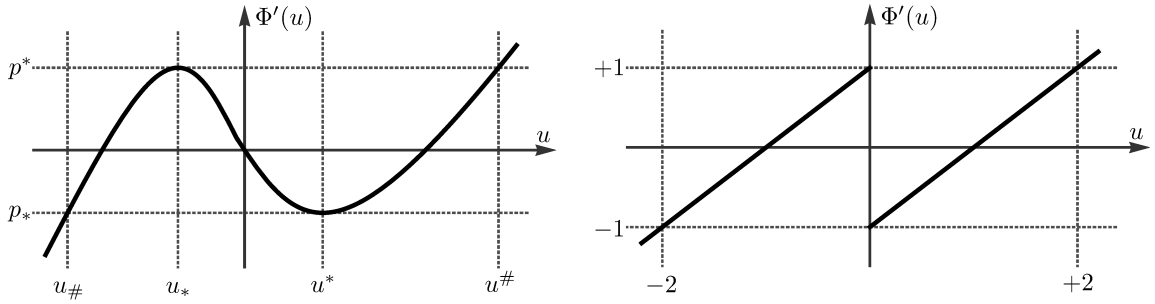

Figure 1.1: *Left.* Bistable derivative of a general double-well potential Φ. The increasing and decreasing branches of Φ' are called *stable* and *unstable*, respectively, while *spinodal region* refers to the interval $[u_*, u^*]$ on which Φ' is decreasing. *Right.* Piecewise affine derivative of the degenerate double-well potential that is studied in §3 and corresponds to $u_\# = -2$, $u_* = u^* = 0$, $u^\# = +2$.

Our goal is to characterize the effective dynamics of (1.1) in the parabolic scaling limit. Interpreting $t \geq 0$ and $j \in \mathbb{Z}$ as the microscopic variables, we introduce the macroscopic time $\tau \geq 0$ and space $\xi \in \mathbb{R}$ by

$$\tau = \varepsilon^2 t, \qquad \xi = \varepsilon j, \tag{1.3}$$

where $\varepsilon > 0$ is a small scaling parameter. We formally identify

$$u_j(t) = U\big(\varepsilon^2 t,\, \varepsilon j\big) \tag{1.4}$$

and aim to describe the evolution of U in the limit $\varepsilon \to 0$. The scaling (1.3) and (1.4) transforms the microscopic dynamics (1.1) into

$$\partial_\tau U = \Delta_\varepsilon\, \Phi'(U), \tag{1.5}$$

where Δ_ε is the standard finite difference approximation of ∂_ξ^2 on $\varepsilon\mathbb{Z}$, so the *naïve continuum limit* as $\varepsilon \to 0$ reads

$$\partial_\tau U = \partial_\xi^2 \Phi'(U). \tag{1.6}$$

This PDE, however, is ill-posed due to the unstable branches of Φ' and can therefore not determine the macroscopic limit of (1.1) completely. Actually, the lattice can be viewed as a *regularization* of (1.6) that accounts for small scale effects and provides in the limit $\varepsilon \to 0$ additional dynamical information such as laws for the motion of phase interfaces or even measure-valued solutions. Other notable regularizations of (1.6) are the Cahn-Hilliard equation

$$\partial_\tau U = \partial_\xi^2 \Phi'(U) - \varepsilon^2 \partial_\xi^4 U, \tag{1.7}$$

which has enjoyed a lot of attention over the last decades, and the viscous approximation

$$\left(1-\varepsilon^2\partial_\xi^2\right)\partial_\tau U=\partial_\xi^2\Phi'(U), \tag{1.8}$$

studied in [NCP91, Plo94, EP04]. As discussed below, the available results indicate that the macroscopic limits of the scaled lattice equation (1.5) and the viscous approximation (1.8) are identical but different from the limit of the Cahn-Hilliard model. In a formal way this can be understood by expanding the spatial operators in powers of ε: Equations (1.1) and (1.8) share (up to a redefinition of ε) the same leading order terms according to

$$\Delta_\varepsilon P=\Big(\partial_\xi^2+\frac{\varepsilon^2}{12}\partial_\xi^4+O\big(\partial_\xi^6\big)\Big)P\,,\qquad \big(1-\varepsilon^2\partial_\xi\big)^{-1}\partial_\xi^2 P=\big(\partial_\xi^2+\varepsilon^2\partial_\xi^4 P+O\big(\partial_\xi^6\big)\big)P,$$

with P being shorthand for $\Phi'(U)$, while (1.7) replaces the right hand side in (1.6) by $\partial_\xi^2 P-\varepsilon^2\partial_\xi^4 U$. For $\varepsilon>0$, however, the rescaled lattice and the viscous approximation are different and it remains open whether there exists a unified theory that is capable of describing the limit $\varepsilon\to 0$ for both models.

A key feature of any regularization of (1.6) with double-well potential Φ are *phase interfaces*, which evolve according to certain jump conditions and separate regions where U attains values in different stable regions (*phases*). Other types of nonconvex potentials give rise to different phenomena such as coarsening of localized spikes, see for instance [EG09].

Numerical simulations of (1.1) as performed in §2 with a generic double-well potential provide evidence for the existence of two different types of phase interfaces. *Type-I interfaces* correspond to piecewise smooth functions U and separate regions where U takes values in either one of the phases $U<u_*$ and $U>u^*$, where $[u_*,u^*]$ is the spinodal interval. *Type-II interfaces*, however, are related to measure-valued solutions of (1.6) and model a phase mixture on at least one side of the interface. For both types, a phase interface can have a fixed position or move, depending on the behavior of $P=\Phi'(U)$ near the interface. While P is smooth across a standing interface and takes values in $[p_*,p^*]=[\Phi'(u^*),\Phi'(u_*)]$, a moving interface is driven by a jump in $\partial_\xi P$ but requires either $P=p_*$ or $P=p^*$ subject to the propagation direction. In the macroscopic limit we therefore find hysteretic behavior in the sense that fronts moving into different phases comply with different constraints, see Figure 1.2. Further intriguing properties of the macroscopic lattice dynamics are sketched in Figure 1.3. Driven by the bulk diffusion, a standing interface can suddenly start to move (*depinning*) and a moving interface can eventually come to rest (*pinning*). Moreover, two interfaces can disappear after a collision (*annihilation*).

Assuming that the lattice data $p_j=\Phi'(u_j)$ converge as $\varepsilon\to 0$ to a sufficiently regular function P and that any phase interface is of type I, the dynamics in the parabolic scaling limit can described by combining bulk diffusion via (1.6) with the generalized Stefan condition

$$[\![P]\!]=0,\qquad \frac{\mathrm{d}\xi^*}{\mathrm{d}\tau}[\![U]\!]+[\![\partial_\xi P]\!]=0 \tag{1.9}$$

and the hysteretic flow rule

$$P=p_*\quad\text{for}\quad\frac{\mathrm{d}\xi^*}{\mathrm{d}\tau}[\![U]\!]>0,\qquad\qquad P=p^*\quad\text{for}\quad\frac{\mathrm{d}\xi^*}{\mathrm{d}\tau}[\![U]\!]<0, \tag{1.10}$$

where $\xi^*(\tau)$ is the position of an interface and $[\![\cdot]\!]$ denotes the jump across this interface. These conditions have also been proposed in [EP04] to model the propagation of type-I interfaces in the limit of the viscous approximation and are naturally related to the notion of *entropy solutions*, see also [MTT09] and the discussion below. For the Cahn-Hilliard equation (1.7), the parabolic scaling limit does not imply any hysteresis. Here each interface corresponds to $P=0$ and evolves therefore according to the classical Stefan condition, see for instance [BBMN12] for a rigorous proof. We also note that there exists at least one other macroscopic limit for (1.7), which is, however, not related

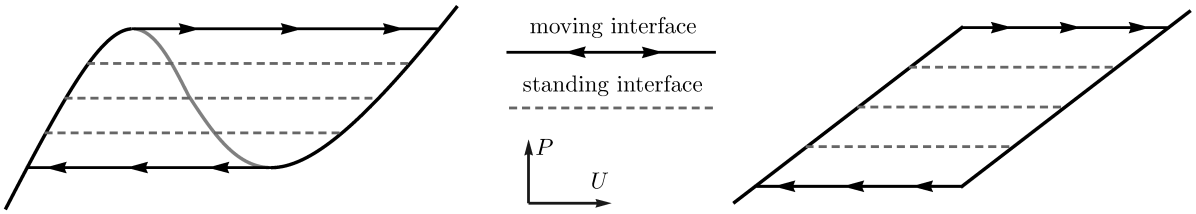

Figure 1.2: *Left.* Cartoon of the macroscopic hysteresis for the potentials from Figure 1.1. The arrows indicate the temporal jump of U when it undergoes a phase transition at a fixed position ξ. In particular, $P = p^*$ holds at any interface that moves into the phase $U < u_*$, whereas propagation into $U > u^*$ requires $P = p_*$. The dashed lines represent standing interfaces, at which P takes values in $[p_*, p^*]$.

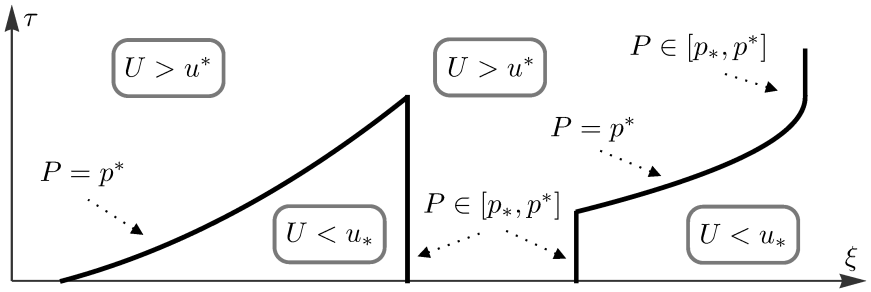

Figure 1.3: Cartoon of three macroscopic type-I interfaces. The first interface (moving) and the second one (standing) eventually collide with each other and disappear (*annihilation*). The third one is initially at rest, starts to move at a later time(*depinning*) and stops eventually again (*pinning*).

to the parabolic scaling (1.3): In the regime of almost vanishing bulk diffusion, interfaces move and merge on a much slower time scale which is exponentially small in ε [ABF91, BH92].

In the case of hysteretic interface motion, there seems to be no rigorous result – neither for the lattice nor the viscous approximation – that derives (1.9) and (1.10) rigorously from the dynamics for $\varepsilon > 0$. Previous results for the lattices (1.1) or (1.2) are either restricted to standing interfaces, see [GN11] and [BGN13] for type-I and type-II interfaces, respectively, or do not capture the dynamics of moving interfaces completely, e. g. [BNP06].

As a first step towards a mathematical justification of the macroscopic evolution laws for type-I interfaces, we study in §3 the special case of

$$\Phi(u) = \tfrac{1}{2} \min\big\{(u-1)^2, (u+1)^2\big\}. \tag{1.11}$$

At the cost of being discontinuous at $u = 0$, the derivative Φ' of (1.11) has two advantages over a generic bistable function. First, the nonlinearity in (1.1) is piecewise affine and second, the spinodal region has shrunk to the point $u = 0$, see the right panel of Figure 1.1. These properties simplify the dynamical system (1.1) significantly and enable us to represent solutions to the nonlinear lattice by a summation formula that involves delayed and shifted versions of the discrete heat kernel.

Due to the degenerate nature of (1.11), it is not our intention to identify the most general class of admissible initial data for which the macroscopic limit can be described by a free boundary problem. On the contrary, in order to keep the presentation as simple as possible, we restrict our considerations in §3 to initial data that produce a single type-I interface which cannot change its direction of propagation. Our main findings are formulated in Theorems 3.2, 3.16, and 3.18, and can informally be summarized as follows.

Main result. *The lattice* (1.1) *with* (1.11) *has the following properties.*

1. Microscopic single-interface solutions*: Type-I interfaces are naturally related to a class of lattice states that is invariant under the dynamics. Specifically, intervals of linear diffusion are*

interrupted by an increasing sequence of phase transition times $(t_k^*)_{k\geq k_1}$ *such that* u_k *switches from negative to positive sign at* $t = t_k^*$.

2. Macroscopic evolution: *When starting with macroscopic single-interface initial data, the limit* $\varepsilon \to 0$ *can be characterized as follows.*

   (a) Convergence*: The lattice data* u_j *converge in a strong sense to a function* U *that is smooth outside of an interface curve* $\tau \mapsto \xi^*(\tau)$*, where* ξ^* *is Lipschitz continuous and nondecreasing. Moreover, the function* $P = U - \operatorname{sgn} U$ *is continuous across the interface.*

   (b) Limit dynamics*: For almost all times* $\tau \geq 0$ *we have either*

$$P(\tau, \xi^*(\tau)) \in [-1, +1] \quad \textit{and} \quad \frac{\mathrm{d}}{\mathrm{d}\tau}\xi^*(\tau) = 0$$

   or

$$P(\tau, \xi^*(\tau)) = +1 \quad \textit{and} \quad \frac{\mathrm{d}}{\mathrm{d}\tau}\xi^*(\tau) > 0,$$

   and P *solves the linear heat equation outside of the interface.*

   (c) Uniqueness*:* U *and* ξ^* *are uniquely determined by the macroscopic initial data and the limit model.*

The rest of the paper is organized as follows. In §2.1 we employ the gradient flow structure of (1.1) to describe the formation of macroscopic data on a heuristic level. Afterwards we report on our numerical investigations for general double-well potentials. We present several examples for the macroscopic motion of type-I and type-II interfaces in §2.2, and proceed in §2.3 with discussing the key features of the microscopic dynamics near moving interfaces. These are: sequentiality of phase transitions, small-scale fluctuations, and existence of multiple time scales. Finally, in §2.4 we give a more detailed description of the macroscopic limit model for type-I interfaces and interpret the hysteretic flow rule in terms of entropy inequalities.

§3 contains our analytical results for the special case (1.11). We first employ ODE arguments in §3.1 in order to prove the persistence of single-interface data. In particular, in Corollary 3.7 we establish the aforementioned representation formula. In §3.2 we then introduce the concept of macroscopic single-interface initial data and derive upper bounds for the macroscopic interface speed from the properties of the discrete heat kernel, see also Appendix A. The main technical work is done in §3.3, were we establish macroscopic compactness results for ξ^* and P in the spaces of Lipschitz and Hölder continuous functions, respectively. In §3.4 we finally pass to the limit $\varepsilon \to 0$. To this end, we first justify the limit model along subsequences, and obtain afterwards both uniqueness and convergence by adapting some arguments from the theory of free boundary problems with hysteresis operators.

2 Heuristic arguments and numerical simulations

In this section we employ heuristic arguments as well as numerical simulations in order to gain a qualitative understanding of the key dynamical features of the nonlinear lattice diffusion with double-well potential. In particular, we discuss (*i*) the underlying gradient flow structure and the formation of macroscopic data during a fast initial transient regime, (*ii*) the microscopic and macroscopic dynamics of phase interfaces, and (*iii*) the macroscopic evolution equations in the limit $\varepsilon \to 0$.

To keep the presentation as simple as possible, we use a finite dimensional lattice with $j = -N, \dots, N$ and close the resulting ODE system by imposing homogeneous Neumann boundary conditions

$$u_{-N-1}(t) = u_{-N}(t)\,, \qquad u_{N+1}(t) = u_N(t). \tag{2.1}$$

The natural scaling parameter on such a finite lattice is $\varepsilon = 1/N$, that means the macroscopic space variable ξ takes values in the interval $[-1,1]$. The numerical simulations presented below are computed by the explicit Euler scheme, where the time step size is chosen sufficiently small so that the energy, see (2.2) below, is strictly decreasing. Moreover, all simulations are performed with

$$\Phi(u) = \frac{2\big(1-u^2\big)^2}{1+u^2}, \qquad \Phi'(u) = 4u - \frac{16u}{(1+u^2)^2},$$

which is convenient for numerical computations since the linear growth of Φ' for $|u| \to \infty$ allows to use a relatively large time-step size.

2.1 Gradient flow structure and onset of macroscopic data

The lattice diffusion (1.1) can be regarded as a discrete analogue to the H^{-1}-gradient flow of a nonlinear bulk energy. More precisely, defining the energy

$$\mathcal{E}(u) := \varepsilon \sum_{j=-N}^{N} \Phi(u_j) \tag{2.2}$$

and the metric potential

$$\mathcal{R}(\dot u) = \frac{\varepsilon}{2} \sum_{j=-N}^{N} \big(\nabla_+ v_j\big)^2 \quad \text{with} \quad -\Delta\, v_j = \dot u_j \quad \text{for} \quad j = -N, \dots, N \quad \text{and} \quad v_{\pm(N+1)} = v_{\pm N}$$

we readily verify – using discrete integration by parts along with the boundary conditions (2.1) – that (1.1) is equivalent to

$$\partial_{\dot u}\mathcal{R}(\dot u) + \partial_u \mathcal{E}(u) = 0,$$

where the metric tensor $\partial_{\dot u}\mathcal{R}$ is formally given by $(-\Delta)^{-1}$. In particular, we obtain the energy balance

$$\frac{\mathrm{d}\mathcal{E}}{\mathrm{d}t} = \varepsilon^2 \frac{\mathrm{d}\mathcal{E}}{\mathrm{d}\tau} = -\varepsilon^2 \mathcal{D}, \qquad \mathcal{D}(u) := \varepsilon^{-1} \sum_{j=-N}^{N} \big(\nabla_+ \Phi'(u_j)\big)^2,$$

where the dissipation $\mathcal{D}$ gives the squared and rescaled length of the energy gradient with respect to the metric induced by $\mathcal{R}$. Notice that $\mathcal{E}$, $\mathcal{R}$, and $\mathcal{D}$ are scaled macroscopically, that means the identification (1.4) implies

$$\mathcal{E}(U) = \int_{-1}^{+1} \Phi(U)\,\mathrm{d}\xi, \qquad \mathcal{D}(U) = \int_{-1}^{+1} \big(\partial_\xi \Phi'(U)\big)^2\,\mathrm{d}\xi \tag{2.3}$$

as well as

$$\mathcal{R}(\partial_\tau U) = \tfrac{1}{2} \int_{-1}^{+1} (\partial_\xi V)^2\,\mathrm{d}\xi \quad \text{with} \quad -\partial_\xi^2 V = \partial_\tau U \quad \text{and} \quad \partial_\xi V|_{\xi=\pm1} = 0 \tag{2.4}$$

provided that U is sufficiently smooth with respect to τ and ξ. The formal gradient flow corresponding to (2.3) and (2.4), however, is the ill-posed PDE (1.6) and can hence not govern the limit dynamics.

A further important observation is that the nonlinear lattice (1.1) admits a comparison principle on the increasing branches of Φ'. Specifically, using standard arguments for ODEs we easily show

$$\sup_{t\geq 0} \sup_{|j|\leq N} u_j(t) \leq \max\big\{u^\#, \sup_{|j|\leq N} u_j(0)\big\}, \qquad \inf_{t\geq 0} \inf_{|j|\leq N} u_j(t) \geq \min\big\{u_\#, \inf_{|j|\leq N} u_j(0)\big\}.$$

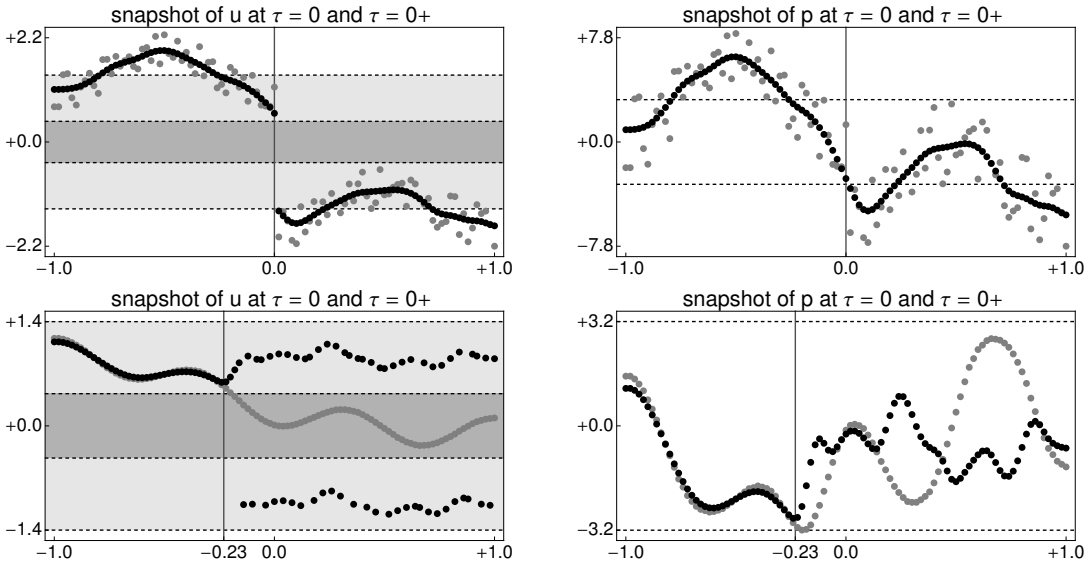

Figure 2.1: Illustration of the initial transient regime for $N = 50$, using snapshots of u_j and p_j (*left* and *right* column, respectively) against $\xi = \varepsilon j$ at time $\tau = 0$ (gray) and a short time $\tau = 0+$ afterwards (black). The shadowed regions in the left column indicate the intervals $[u_*, u^*]$ and $[u_\#, u^\#]$; the dotted horizontal lines in the right column represent the critical values $\{p_*, p^*\}$. The vertical lines describe the macroscopic phase interfaces. *Top row.* In this example, the initial data $u_j(0)$ at $\tau = 0$ do not penetrate the spinodal interval. The lattice data u_j and p_j at $\tau = 0+$ therefore resemble macroscopic functions U and P, which are discontinuous and continuous, respectively, at the phase interface. *Bottom row.* Part of the initial data $u_j(0)$ are now taken from the spinodal interval. At time $\tau = 0+$, the lattice data u_j can no longer be described by macroscopic functions but only by Young measures. The data p_j, however, still approximate a continuous macroscopic function P.

This implies $\mathcal{E}(t) = O(\varepsilon N) = O(1)$ for all $t \geq 0$ and hence $\int_0^\infty \mathcal{D}(u(t))\,\mathrm{d}t = O(1)$ provided that the initial data $u_j(0)$ are bounded independently of ε.

We next discuss the small-time dynamics. For $0 < \varepsilon \ll 1$ the initial evolution of (1.1) is related to a very fast transient regime – where 'fast' refers to the macroscopic time τ – during which the system quickly approaches a state with macroscopic behavior of p_j and dissipation of order $O(1)$. This is illustrated in Figure 2.1, which depicts two prototypical examples of initial data at $\tau = 0$ along with the state of the system at a small macroscopic time $\tau = 0+$ afterwards.

In the top row of Figure 2.1, we start with microscopic (i. e., oscillatory) initial data that are confined to the two stable regions $u \in (-\infty, u_*)$ and $u \in (u^*, +\infty)$. Due to the oscillations, the initial dissipation is of order $O(\varepsilon^{-1}N) = O(\varepsilon^{-2})$. The initial energy gradient is therefore also very large and drives the system rapidly. At time $\tau = 0+ \approx O(\varepsilon^2)$, the dissipation and the energy gradient eventually become of order $O(1)$. This implies that the discrete data p_j resemble a macroscopic function P that admits a weak spatial derivative and is hence continuous with respect to ξ. We also observe that the discrete data u_j at $\tau = 0+$ approximate a piecewise continuous function U which satisfies $P = \Phi'(U)$ and jumps across the interface located at $\xi = 0$. In particular, the *phase fraction* μ defined by

$$\mu := \chi_{[u^*,+\infty)}(U) - \chi_{(-\infty,u_*)}(U)$$

takes the values -1 and $+1$ outside of the interface, where χ_J denotes the indicator function of the interval J.

The second example, see the bottom row in Figure 2.1, is different since now some of the initial data $u_j(0)$ belong to the spinodal interval $[u_*, u^*]$, in which the discrete diffusion coefficient is negative. In the numerical simulation we therefore observe that each of those u_j quickly leaves the spinodal interval (*spinodal decomposition*) and that the data for adjacent j can be attracted by different stable regions. In particular, the data at time $\tau = 0+ \approx O(\varepsilon^2)$ exhibit a phase interface near

$\xi \approx -0.23$, in the sense that u_j is non-oscillatory on the left but highly oscillatory on the right of the interface. The fine structure of these oscillations depends on the microscopic details and each reasonable macroscopic theory must describe them in terms of a Young measure $\nu = \nu(\tau, \xi, \mathrm{d}u)$, which provides a probability distribution with respect to u for any macroscopic point (τ, ξ). The discrete data p_j, however, still resemble a macroscopic function P because otherwise the dissipation could not be of order $O(1)$. Since p_j and u_j are coupled by Φ', we then conclude that the u-support of the Young measure ν consists of only two points. This reads

$$\nu(\tau, \xi, \mathrm{d}u) = \frac{1 - \mu(\tau, \nu)}{2} \delta_{\beta_-(P(t,\xi))}(\mathrm{d}u) + \frac{1 + \mu(\tau, \nu)}{2} \delta_{\beta_+(P(t,\xi))}(\mathrm{d}u). \tag{2.5}$$

Here, $\delta_\beta(\mathrm{d}u)$ is the Dirac distribution at β, the functions β_-, β_+ denote the two stable branches of the inverse of Φ', and the phase fraction μ takes values in $[-1, +1]$.

The simulations from Figure 2.1 reveal that there exist (at least) two different types of macroscopic phase interfaces: Type-I interfaces separate regions where the microscopic data u_j are confined to either one of the phases $(-\infty, u_*)$ and $(u^*, +\infty)$, whereas type-II interfaces describe that the lattice data oscillate between the two phases on at least one side of the interface. Below we argue that type-I interfaces can be described by a free boundary value problems, which exhibits hysteresis and involves only the macroscopic fields P and $\mu \in \{-1, +1\}$. Type-II interfaces, however, are more complicated and their investigation is postponed to future research.

2.2 Examples of macroscopic interface dynamics

In this section we study the dynamics of type-I interfaces in numerical simulations. In particular, we investigate the macroscopic jump conditions across such interfaces and provide numerical evidence for pinning, depinning, and annihilation. At the end we also present an example of a type-II interface.

For simplicity, and in view of the discussion in the previous section, we always impose initial data $u_j(0)$ such that $p_j(0) = \Phi'(u_j(0))$ resemble a macroscopic function $\xi \mapsto P(0, \xi)$. In all simulations we observe – for, loosely speaking, most of the macroscopic times $\tau > 0$ – that the discrete data $p_j(\tau/\varepsilon^2)$ approximate a macroscopic function $\xi \mapsto P(\tau, \xi)$. We therefore expect that the macroscopic limit $\varepsilon \to 0$ can in fact be characterized by a PDE for P and the phase field μ, or equivalently, in terms of a free boundary problem for $P = \Phi'(U)$ and the interface curves. There exist, however, small macroscopic times intervals in which the discrete data $p_j(t)$ exhibit strong temporal and spatial fluctuations near a moving phase interface. These fluctuations are discussed in the next section.

Figure 2.2 depicts lattice simulations with two different values of N, showing that the macroscopic plots of the discrete data are basically independent of N. In this example, we initialize two macroscopic phase interfaces which are located at $\xi = 0$ and $\xi = 0.6$ and separate regions with $U > u^\#$, $U \in [u_\#, u_*]$, and $U \in [u^*, u^\#]$. The first interface moves to the right while the second one clearly keeps its initial position. At the later time $\tau \approx 0.18$ both interfaces annihilate each other in a collision process, see also Figure 2.4, and the macroscopic evolution afterwards is governed by nonlinear diffusion inside the phase $U \in [u^*, \infty)$. Figure 2.3 provides numerical evidence for the jump rules across the interface: The moving interface is driven by a jump in $\partial_\xi P$ whereas P is smooth across the standing interface. Moreover, while $P = p^*$ holds on the moving interface, P evolves on the standing interface and takes values in $[p_*, p^*]$.

A further dynamical feature of the lattice (1.1), namely the pinning of interfaces, is illustrated in Figure 2.5. At time $\tau = 0$, we initialize a single macroscopic interface that separates regions with $U \geq u^*$ and $U \in [u_\#, u_*]$, where the data are chosen such that $P > p^*$ and $P < p^*$ holds locally on the left and on the right of the interface, respectively. This interface starts propagating to the right but stops moving at $\tau \approx 0.02$ because the bulk diffusion behind the interfaces enforces $P \leq p^*$ for $\tau \gtrsim 0.02$. The inverse process, that is the depinning of interfaces, is shown in Figure 2.6. There, a single macroscopic interface is initially at rest with $P \in (p_*, p^*)$ but propagates with $P = p^*$ for $\tau \gtrsim 0.03$.

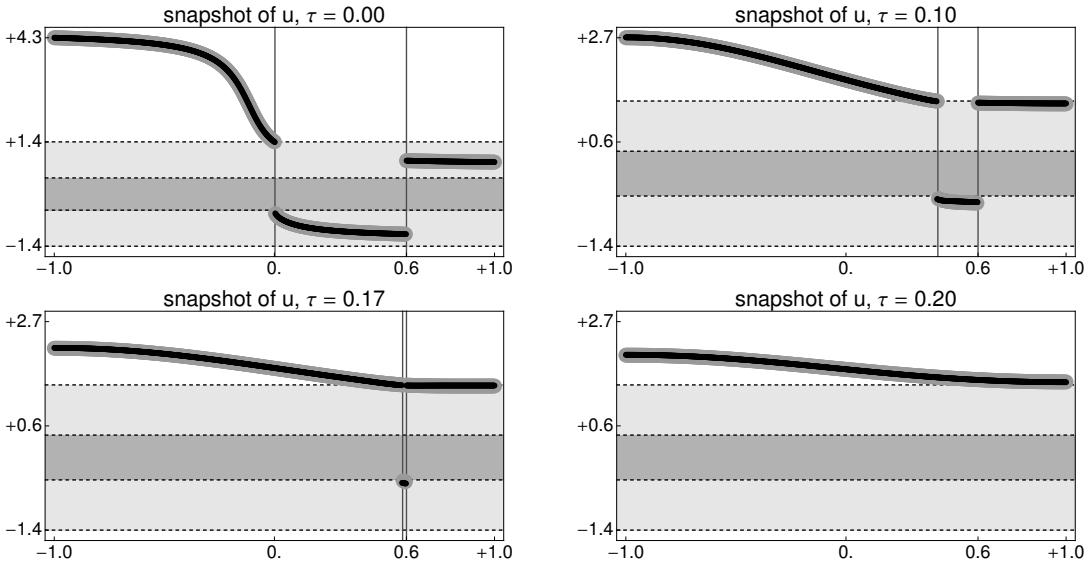

Figure 2.2: Annihilation of a moving and a standing type-I interface for two different simulations with $N = 200$ (thick gray curves) and $N = 500$ (thin black curves). The snapshots show u_j against the macroscopic position $\xi = \varepsilon j$ at fixed macroscopic times τ; the vertical lines indicate the interface positions and the two shaded regions represent the intervals $[u_*, u^*]$ and $[u_\#, u^\#]$.

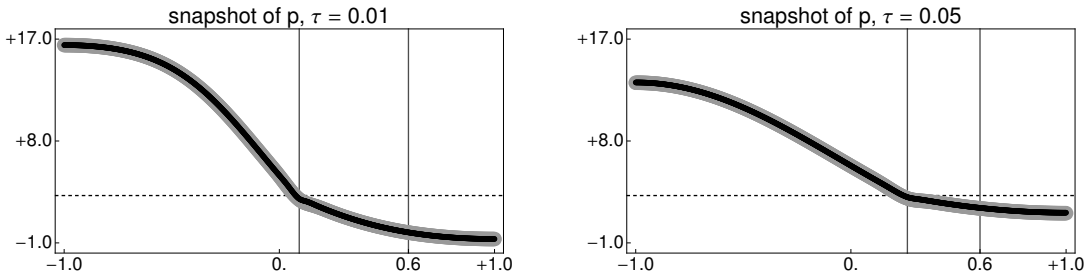

Figure 2.3: Snapshots of p_j for the example from Figure 2.2. The horizontal line represents $p = p^*$.

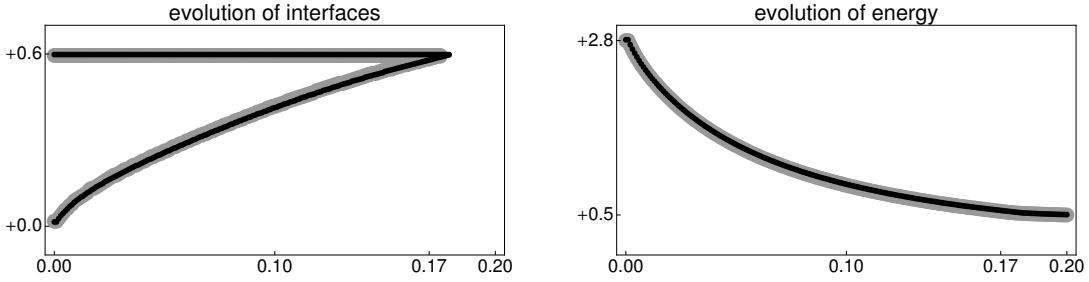

Figure 2.4: Macroscopic positions of the interfaces and the energy as function of τ for the example from Figure 2.2.

The last example is shown in Figure 2.7 and concerns the dynamics of type-II interfaces. The discrete initial data $u_j(0)$ resemble a smooth function U that penetrates the spinodal region, and the initial transient regime therefore leads to spinodal decomposition. This means the lattice dynamics forms a phase interface that separates a region with $U > u_*$ from a region with strong microscopic oscillations, where the latter can be regarded as an approximation of a nontrivial Young measure ν. The interface is initially at rest but depins at $\tau \approx 0.02$ and propagates into the oscillatory phase afterwards. The dynamics of type-II interfaces are not yet well-understood. In particular, since there exist many microscopic realizations of a given Young measure ν, it is not clear whether the macroscopic evolution can be completely characterized in terms of the fields P and $\mu \in [-1, +1]$,

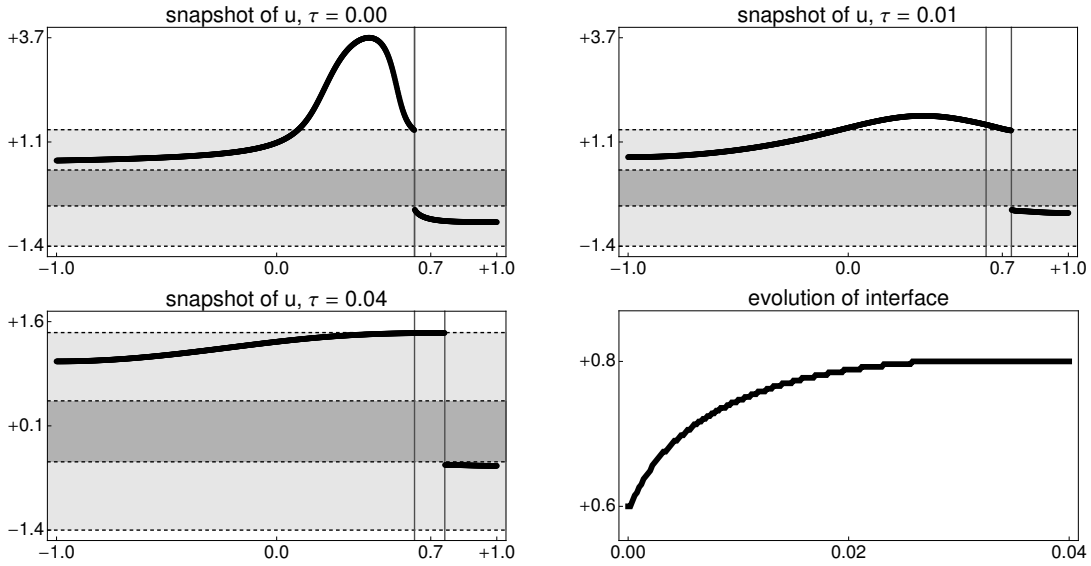

Figure 2.5: Pinning of a type-I interface with $N = 400$. The vertical lines indicate the initial and the current position of the interface.

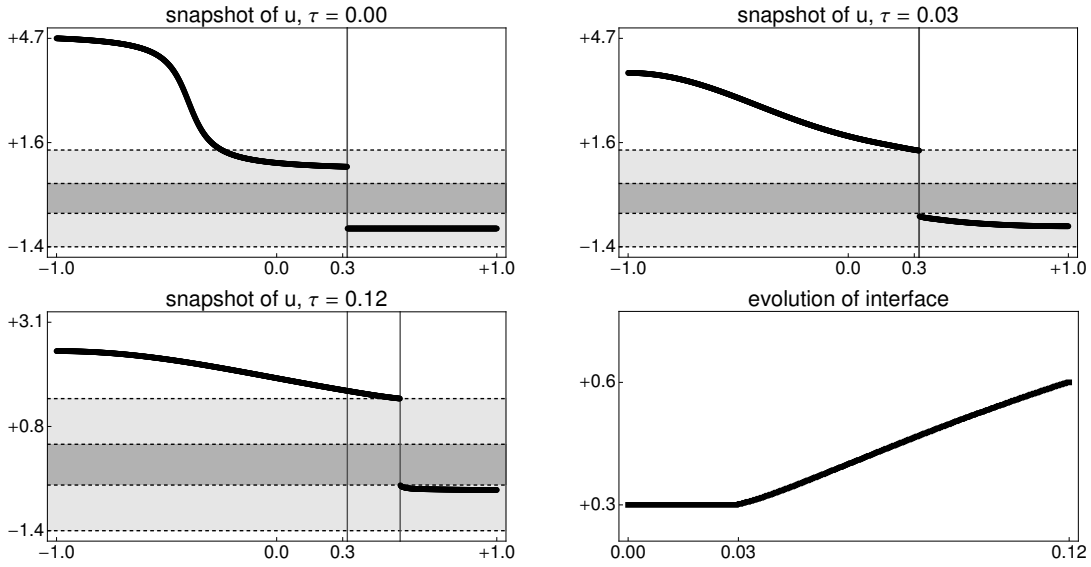

Figure 2.6: Depinning of a type-I interface with $N = 500$.

or whether further macroscopic quantities are needed. All subsequent considerations are therefore restricted to type-I interfaces.

2.3 Microscopic dynamics of phase interfaces

To conclude our numerical investigations, we now discuss the microscopic dynamics of moving type-I interfaces in greater detail. In this way we not only obtain a better understanding of the lattice dynamics but also gain some inside into the analytical problems that must be addressed when passing to the limit $\varepsilon \to 0$.

For a moving type-I interface that is isolated – i. e., sufficiently far from any other interface and the boundary of the computational domain – the key numerical observations are illustrated in Figures 2.8 and 2.9 and can be summarized as follows.

1. *Sequentiality.* At each time there exists at most one index k such that u_k is inside the spinodal interval $[u_*, u^*]$. In other words, the interface moves because the u_j's undergo the phase transition *one after another*, where 'phase transition' means passage through the spinodal interval.

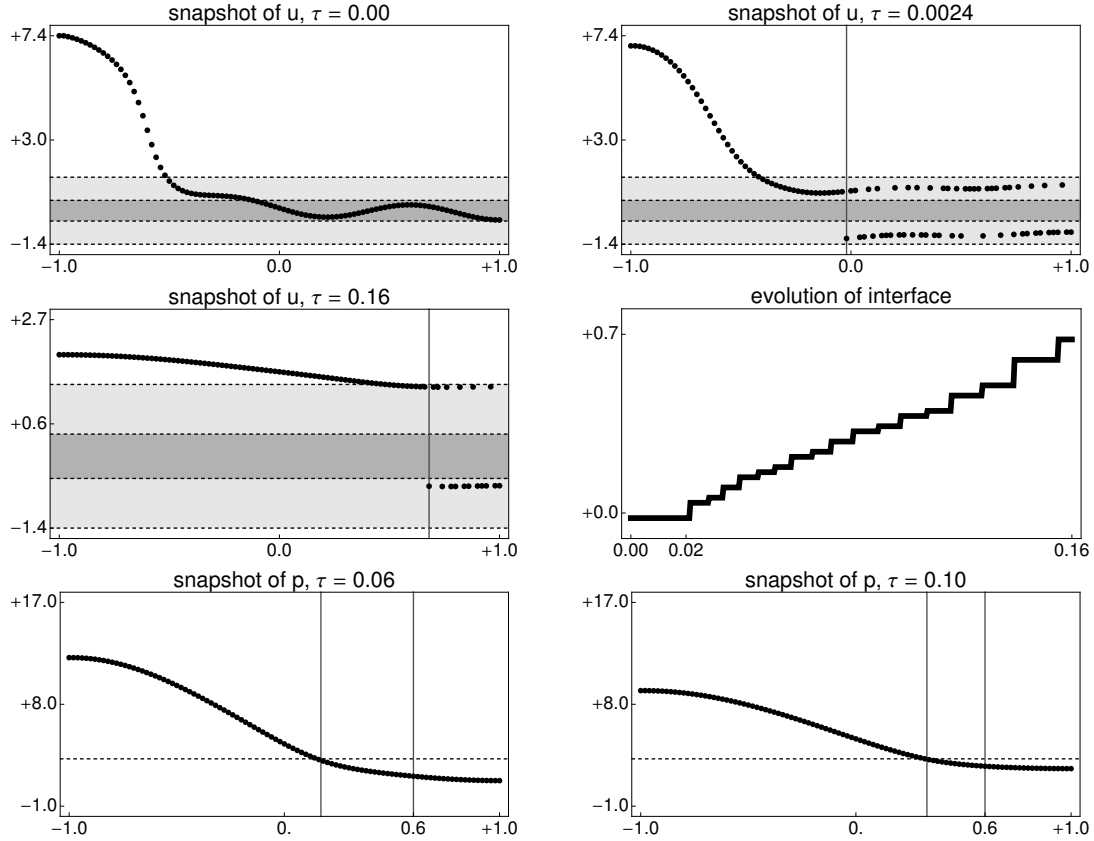

Figure 2.7: Type-II interface with $N = 50$ that propagates into a region with microscopic oscillations. In the macroscopic limit, these oscillations cannot be described by a function U but only in terms of a Young measure ν, see 2.5.

2. *Fluctuations near the interface.* Each phase transition produces strong microscopic fluctuations. These fluctuations are initially very localized, correspond to relatively large dissipation, and are spread out before the next phase transition occurs.

3. *Temporal scale separation.* The time needed to spread out the fluctuations is as least as large as the time to undergo a phase transition. Moreover, both times are typically much smaller than the time between two subsequent phase transition.

The fundamental sequentiality property can – at least in an idealized single-interface setting – be derived from elementary comparison principles for ODEs. The underlying idea is that as long as u_k is inside of $[u_*, u^*]$, the lattice equation ensures that any other u_j cannot enter the spinodal interval. For the piecewise quadratic potential, we employ a similar argument in the proof of Theorem 3.2 in order to show the persistence of single-interface data.

The microscopic fluctuations are much harder to describe rigorously. More precisely, although it is relatively simple to understand the onset of fluctuations heuristically, it is not obvious, at least to the authors, how to estimate their spatial and temporal decay in the case of a generic double-well potential Φ. For the piecewise quadratic potential, however, the fluctuations can be controlled by splitting $p = \Phi'(u)$ into a regular part related to linear diffusion and a sum over delayed and shifted variants of the discrete heat kernel, see the discussion in §3.

A further challenge for any rigorous treatment is to give a suitable description of the different time scales in the problem. For instance, in order to guarantee that each interface propagates with finite speed on the macroscopic scale, one has to show that the microscopic time between two adjacent phase transitions is of order $O(\varepsilon^{-1})$. Moreover, proving that any limit function P is in fact continuous at the interface requires to show that both the time for each phase transition and the decay time of the fluctuations are much smaller than $O(\varepsilon^{-1})$. For piecewise quadratic Φ, the problem is again

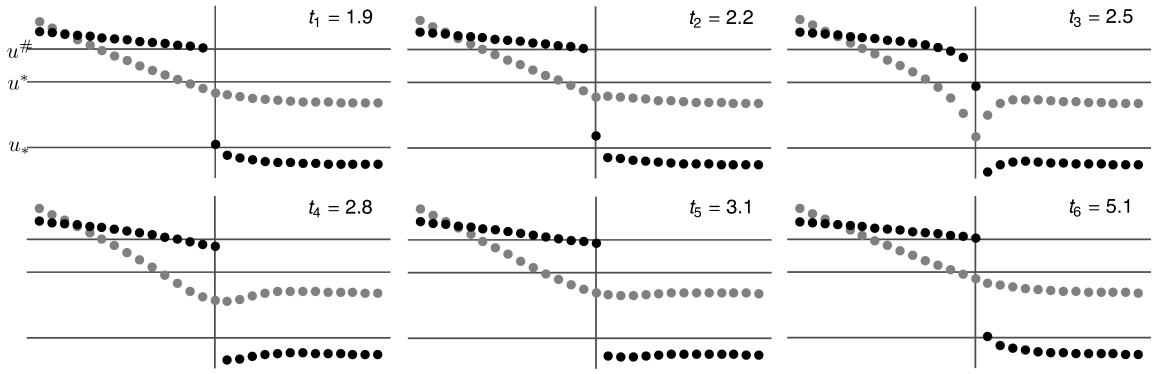

Figure 2.8: Microscopic dynamics of a moving type-I interface: snapshots of $u_j(t)$ (black) and p_j (gray, rescaled) against $j \in \mathbb{Z}$ at six non-equidistant times; the vertical line indicates the interface position at $j = k$. At time t_1, the value u_k has just crossed u_* from below. Afterwards, it passes rapidly through the spinodal interval $[u_*, u^*]$ and evokes microscopic fluctuations which are of order 1 but localized near $j \approx k$. At time t_3, the value u_k leaves the spinodal interval but the fluctuations are still present and not spread out before the time t_5. Between t_5 and t_6, the data change only little but prepare u_{k+1} for the next phase transition, that means $u_k(t_6) > u^*$ and $u_{k+1}(t_6) = u_*$.

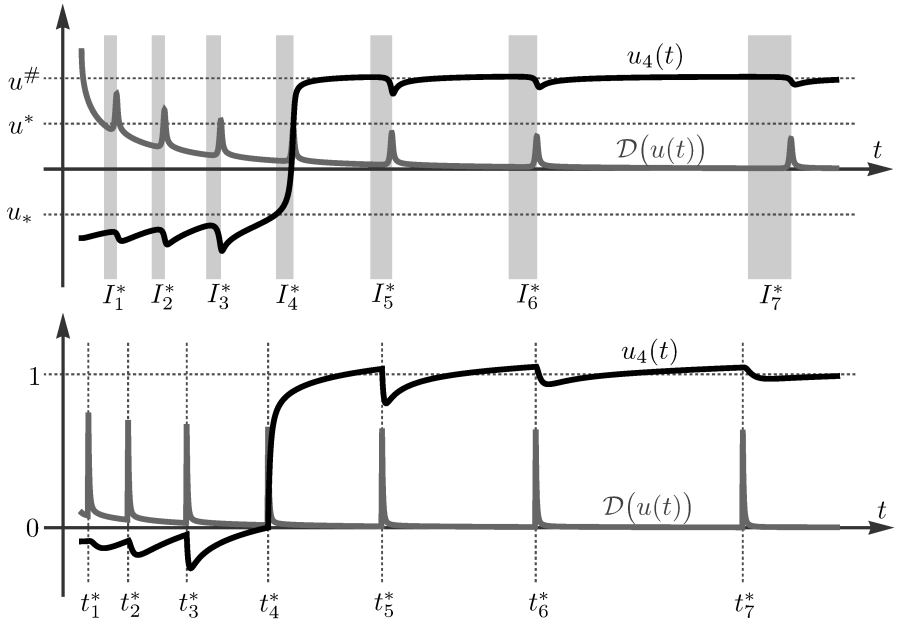

Figure 2.9: Microscopic dynamics of a type-I interface that moves from $j = 1$ to $j = 8$. The black curves represent the time trajectory of u_4, and the gray curves describe the (rescaled) dissipation of the system. *Top.* Φ is a smooth double well-potential and each interval I_k^* contains all times at which u_k is inside of the spinodal interval. *Bottom.* For the piecewise quadratic potential, each interval I_k^* is degenerate and consists of a single time t_k^* with $u_k(t_k^*) = 0$.

much simpler. At first, phase transitions take place at precise times due to the degenerate spinodal region, and second, all other time scales can be related to the properties of the discrete heat kernel.

2.4 Effective evolution equations for the macroscopic dynamics

We now derive the free boundary problem for the dynamics of type-I interfaces on a heuristic level. Since our arguments are very similar to those for the viscous approximation, we only sketch the main ideas and refer to [EP04] for more details.

We first suppose that the lattice data u_j and p_j converge strongly as $\varepsilon \to 0$ to macroscopic functions U and P which are sufficiently regular. For simplicity we also assume that there is only a

single interface located at $\xi^*(\tau)$ and that U satisfies the *phase condition*

$$U > u^* \quad \text{for} \quad \xi < \xi_* \quad \text{an} \quad U < u_* \quad \text{for} \quad \xi > \xi_*. \tag{2.6}$$

Under these assumptions, and using the weak formulation of (1.5), we readily verify that that macroscopic evolution is governed by *bulk diffusion* via

$$\partial_\tau U = \partial_\xi^2 P \quad \text{with} \quad P = \Phi'(U) \quad \text{for all} \quad \tau \geq 0, \;\; \xi \neq \xi^*(\tau) \tag{2.7}$$

and the *generalized Stefan condition*

$$[\![P]\!] = 0 \quad \text{and} \quad \frac{\mathrm{d}\xi^*}{\mathrm{d}\tau}[\![U]\!] + [\![\partial_\xi P]\!] = 0 \qquad \text{for} \quad \xi = \xi^*(\tau), \tag{2.8}$$

which ensures that (2.7) holds in a distributional sense even across of the interface. Here $[\![U]\!]$ denotes as usual the jump of U across the interface, this means

$$[\![U]\!](\tau) = U_+(\tau) - U_-(\tau), \qquad U_\pm(\tau) := \lim_{h \searrow 0} U(\tau, \, \xi^*(\tau) \pm h).$$

The nontrivial part is to identify a further dynamical interface condition since (2.7) and (2.8) do not the determine the evolution of ξ^* completely. In view of the numerical results, we propose the following *hysteretic flow rule*, see Figures 1.2 and 1.3: At almost each time $\tau > 0$, the interface is either

1. *standing* with $[\![P]\!] = [\![\partial_\xi P]\!] = \frac{\mathrm{d}}{\mathrm{d}\tau}\xi^* = 0$ and $P \in [p_*, p^*]$, or
2. *propagating into* $U < u_*$ with $P = p^*$, $\frac{\mathrm{d}}{\mathrm{d}\tau}\xi^* > 0$, and $[\![U]\!] = u_* - u^\# < 0$, or
3. *propagating into* $U > u^*$ with $P = p_*$, $\frac{\mathrm{d}}{\mathrm{d}\tau}\xi^* < 0$, and $[\![U]\!] = u_\# - u^* < 0$.

Notice that the combination of phase condition, bulk diffusion, Stefan condition, and flow rule provides – at least on a formal level – a well-posed free boundary value problem and that the limit model can easily be generalized to an interface with $U < u_*$ for $x < \xi_*$ and $U > u^*$ for $\xi > \xi_*$, and to the case of finitely many phase interfaces.

The interface laws can also be derived in a more sophisticated way. For the viscous approximation, it has been shown in [EP04] – also assuming sufficiently strong convergence as $\varepsilon \to 0$ – that any limit solution must satisfy the distributional *entropy condition*

$$\partial_\tau \Psi(U) - \partial_\xi\big(\Upsilon(P)\partial_\xi P\big) \leq 0 \tag{2.9}$$

where Υ is an arbitrary but increasing function and Ψ defined by $\Psi'(U) = \Upsilon\big(\Phi'(U)\big)$. This family of local entropy inequalities can also be established in the lattice case. In fact, the scaled equation (1.5) implies

$$\partial_\tau \Psi(U) = \Upsilon(P)\, \Delta_\varepsilon P = \nabla_{+\varepsilon}\Big(\Upsilon(P)\nabla_{-\varepsilon}P\Big) - \big(\nabla_{+\varepsilon}\Upsilon(P)\big)\big(\nabla_{+\varepsilon}P\big) \leq \nabla_{+\varepsilon}\Big(\Upsilon(P)\nabla_{-\varepsilon}P\Big)$$

due to $\Upsilon' \geq 0$, and passing to $\varepsilon \to 0$ in the weak formulation of (1.5) we get (2.9). The key observation is that (2.9) combined with (2.8) yields

$$\frac{\mathrm{d}\xi^*}{\mathrm{d}\tau}\Big([\![\Psi(U)]\!] - \Upsilon(P)[\![U]\!]\Big) \leq 0 \qquad \text{and hence} \qquad \frac{\mathrm{d}\xi^*}{\mathrm{d}\tau}\left(\int_{U_-}^{U_+} \Upsilon\big(\Phi'(s)\big) - \Upsilon(P)\,\mathrm{d}s\right) \leq 0,$$

where $U_- > U_+$ and $P_- = P_+ = P$ hold thanks to (2.6) and (2.8). The flow rule now follows from evaluating the latter inequality for appropriately chosen functions Υ, see again [EP04] for the details.

In the special case that Φ is given by the piecewise quadratic potential (1.11), the bulk diffusion can be written as

$$\partial_\tau P = \partial_\xi^2 P \quad \text{for all} \quad \tau \geq 0, \;\; \xi \neq \xi^*(\tau),$$

whereas the Stefan condition simplifies to

$$[\![P]\!] = 0 \quad \text{and} \quad 2\frac{\mathrm{d}}{\mathrm{d}\tau}\xi_* = [\![\partial_\xi P]\!] \qquad \text{for} \quad \xi = \xi^*(\tau).$$

In the space of distributions, both equations can be combined to

$$\partial_\tau(P+\mu) = \partial_\xi^2 P \qquad \text{for all} \quad \tau \geq 0, \;\; \xi \in \mathbb{R}, \tag{2.10}$$

where the phase field

$$\mu(\tau,\, \xi) := \operatorname{sgn}\big(\xi^*(\tau) - \xi\big) \tag{2.11}$$

is well-defined outside of the interface and takes values in $\{-1, +1\}$. We mention that the hysteretic flow rule can be encoded as

$$\mu = \mathcal{M}[P] \tag{2.12}$$

where $\mathcal{M}$ is a particular *relay operator*, see for instance [Vis94, BS96], and that well-posedness of the initial value problem for (2.10) and (2.12) has been proven in [Vis06]. For our purposes, however, the differential relations from above are more convenient than the discontinuous hysteresis operator $\mathcal{M}$. In particular, under the sharpened phase condition

$$U(\tau,\, \xi) \geq u_\# = -2 \qquad \text{for} \qquad \xi > \xi^*(\tau),$$

which implies that the interface is either at rest or propagates to the right, the flow rule is equivalent to

$$P\big(\tau,\, \xi^*(\tau)\big) \in [-1, +1] \quad \text{with} \quad P\big(\tau,\, \xi^*(\tau)\big) = +1 \quad \text{for} \quad \frac{\mathrm{d}\xi^*}{\mathrm{d}\tau}(\tau) > 0. \tag{2.13}$$

In §3 we prove that the simplified free boundary value problem (2.10) with (2.11) and (2.13) indeed governs the parabolic scaling limit of (1.1) with (1.11) provided that we impose macroscopic single-interface initial data as described in Assumption 3.6.

3 Rigorous analysis for the piecewise quadratic potential

In this section we characterize the lattice dynamics with piecewise quadratic potential. In particular, from now on we suppose that

$$\Phi'(u) = u - \operatorname{sgn} u, \tag{3.1}$$

where we define the sign function by

$$\operatorname{sgn} u = \begin{cases} -1 & \text{for} \quad u < 0, \\ +1 & \text{for} \quad u \geq 0. \end{cases} \tag{3.2}$$

The condition $\operatorname{sgn} 0 = +1$ is essential for establishing global existence and uniqueness of single-interface solutions, see the proof of Theorem 3.2 and the remark afterwards.

Our goal in this section is to prove (i) that a certain class of well-prepared microscopic initial data give rise to a single phase interface that moves in a certain direction, and (ii) that the macroscopic dynamics for $\varepsilon \to 0$ can in fact be described by the simplified free boundary problem from §2.4.

3.1 Existence of single-interface solutions

In order to make precise what we mean by single-interface solution, we define for each $k \in \mathbb{Z}$ the state space

$$X_k = \Big\{ u \in \ell^\infty(\mathbb{Z}) \ : \quad 0 < \inf_{j<k} u_j \le \sup_{j<k} u_j < \infty, \quad -2 < \inf_{j\ge k} u_j \le \sup_{j\ge k} u_j < 0 \Big\},$$

see Figure 3.1 for an illustration. As shown below, the dynamics for initial data chosen from X_k is as follows: The system stays inside X_k until some maximal time $t_k^* > 0$ with $\lim_{t\to t_k^*} u_k(t) = 0$ at which u_k undergoes a phase transition by crossing the spinodal value 0 from below. For times $t > t_k^*$, the system evolves inside of X_{k+1} until u_{k+1} changes from negative to positive phase at time $t_{k+1}^* > t_k^*$. By iteration we therefore find a phase interface that moves to the right, where we allow for $t_k^* = \infty$ to account for standing interfaces.

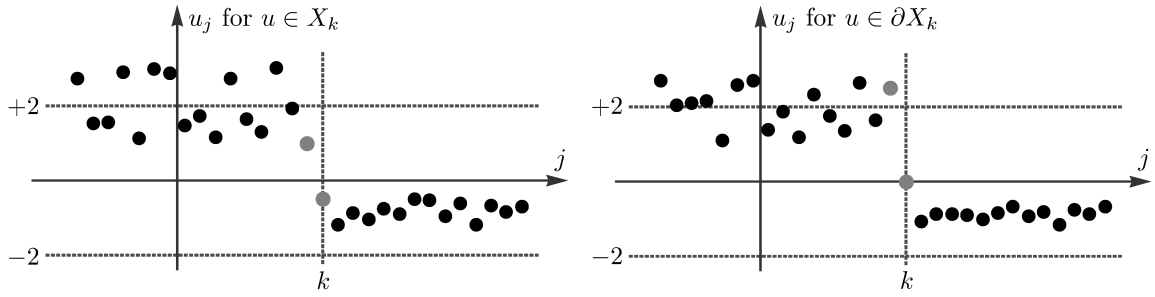

Figure 3.1: States from X_k have a single phase interface at k (*left panel*, u_{k-1} and u_k are highlighted). Under the dynamics, this interface is either stationary for all times or shifts eventually to the right due to a phase transition of u_k, because the system can reach the boundary ∂X_k only via $u_k = 0$. When this happens at time t_k^* (*right panel*), we also have $u_{k-1}(t_k^*) > 2$ and $\dot{u}_k$ jumps from $\dot{u}_k(t_k^* - 0) \ge 0$ to $\dot{u}_k(t_k^* + 0) \ge 4$. Afterwards the state of the system belongs to X_{k+1} until u_{k+1} undergoes a phase transition at time t_{k+1}^*.

Definition 3.1 (single-interface solution)**.** A continuous function $u\colon [0,\infty) \to \ell^\infty(\mathbb{Z})$ is called *single-interface solution* to (1.1) with potential (3.1) if there exists $k_1 \in \mathbb{Z}$ along with a sequence $(t_k^*)_{k\ge k_1} \subset (0,\infty]$ such that the following conditions are satisfied with $t_{k_1-1}^* := 0$:

1. For all $k \ge k_1$, we have either $t_{k-1}^* = \infty$ or $t_{k-1}^* < t_k^*$,
2. The function u solves $\dot{u}_j = \Delta\, \Phi'(u_j)$ for all times $t \in [0,\infty) \setminus \{t_k^* : k \ge k_1\}$,
3. We have $u_k(t_k^*) = 0$ and $\lim_{t\searrow t_k^*} \dot{u}_k(t) > 0$ for all $k \ge k_1$ with $t_k^* < \infty$,
4. The function u takes values in X_k on each time interval (t_{k-1}^*, t_k^*) with $t_{k-1}^* < \infty$.

Moreover, a single-interface solution with $t_k^* = \infty$ for all $k \ge k_1$ is called a *standing-interface solution*.

For single-interface solutions in the sense of Definition 3.1, any u_k is continuous at the phase transition time t_k^*, whereas p_k jumps at t_k^* from $+1$ to -1. Notice that it is the other way around in the macroscopic limit: when ε tends to 0, p becomes continuous with respect to both τ and ξ, whereas u jumps from 0 to $+2$ at the phase interface, see Figure 2.9 for an illustration.

As first main result we prove that single-interface solutions exist.

Theorem 3.2 (existence and uniqueness of single-interface solutions)**.** *For given initial data in X_{k_1}, there exists a unique single-interface solution to* (1.1) *with* (3.1)*. Moreover, this solution satisfies*

$$\sup_{t\in[0,\infty)} \sup_{j\in\mathbb{Z}} u_j(t) \le D := \max\big\{2, \sup_{j\in\mathbb{Z}} u_j(0)\big\},$$

and we have

$$u_{k-1}(t_k^*) > 2, \qquad t_{k+1}^* - t_k^* \geq \ln \sqrt{\frac{D+2}{D-2}}, \qquad \dot{u}_k(t_k^*) = \lim_{t \searrow t_k^*} \dot{u}_k(t) = 4 + \lim_{t \nearrow t_k^*} \dot{u}_k(t) \geq 4$$

for all $k \geq k_1$ with $t_k^* < \infty$.

Proof. We assume, without loss of generality, that $k_1 = 1$ and derive all claims by induction with respect to $k \geq k_1$.

Dynamics inside of X_1: For states $u \in X_1$ we have $\operatorname{sgn} u_j = -\operatorname{sgn}(j-1)$ and hence

$$\dot{u}_j = \Delta\, \Phi'(u_j) = \Delta\, u_j + 2\delta_j^0 - 2\delta_j^1, \tag{3.3}$$

where δ_j^k is the Kronecker delta. In particular, the right hand side of (3.3) is Lipschitz continuous with respect to the ℓ^∞-norm of u and this implies the local existence of a unique solution that is smooth in time and takes values in the open set X_1. From the definition of X_1 we also infer that

$$\begin{array}{rcll} 0 & \leq & \dot{u}_j(t) + 2u_j(t) & \leq & 2D & \text{for } j < 1, \\ 0 & \leq & \dot{u}_j(t) + 2u_j(t) & \leq & D+2 & \text{for } j = 0, \\ -4 & \leq & \dot{u}_j(t) + 2u_j(t) & & & \text{for } j = 1, \\ -4 & \leq & \dot{u}_j(t) + 2u_j(t) & \leq & 0 & \text{for } j > 1, \end{array}$$

and the comparison principle for scalar ODEs gives

$$\begin{array}{rcccl} e^{-2t}u_j(0) & \leq & u_j(t) & \leq & e^{-2t}u_j(0) + \big(1 - e^{-2t}\big)D & \text{for } j < 1, \\ e^{-2t}u_j(0) - 2\big(1 - e^{-2t}\big) & \leq & u_j(t) & & & \text{for } j \geq 1, \\ & & u_j(t) & \leq & e^{-2t}u_j(0) & \text{for } j > 1. \end{array}$$

Using these estimates, we now conclude that the local solution with values in X_1 either exists for all times (in which case we set $t_1^* := \infty$) or reaches the boundary of X_1 at some time $0 < t_1^* < \infty$ via $u_1(t_1^*) = 0$. Moreover, since both u_1 and $\dot{u}_1$ are continuous at any $t \in [0, t_1^*)$ we have $\lim_{t \nearrow t_1^*} \dot{u}_1(t) \geq 0$.

Phase transition at t_1^*: Now suppose that $t_1^* < \infty$. From (3.3) and the above estimate for $u_j(t)$ we conclude that $u_j(t)$ converges for any $j \in \mathbb{Z}$ as $t \nearrow t_1^*$ to some well-defined limit $u_j(t_1^*)$, where $u_1(t_1^*) = 0$ as well as

$$0 < \inf_{j<1} u_j(t_1^*) \leq \sup_{j<1} u_j(t_1^*) < D, \qquad -2 < \inf_{j>1} u_j(t_1^*) \leq \sup_{j>1} u_j(t_1^*) < 0.$$

We therefore have

$$\sup_{j \in \mathbb{Z}} \big| \Delta\, \Phi'\big(u_j(t_1^*)\big) \big| \leq C$$

for some constant C. On the other hand, $u_0(t_1^*) > 0$ and $-2 < u_2(t_1^*) < 0$ ensure that

$$\Delta\, \Phi'\big(u_1(t_1^*)\big) = \Big(u_0(t_1^*) + u_2(t_1^*)\Big) - \Big(\operatorname{sgn} u_0(t_1^*) + \operatorname{sgn} u_2(t_1^*) - 2\operatorname{sgn} 0\Big) > 0$$

thanks to $\operatorname{sgn} 0 = +1$. These results reveal that the vector field of the dynamical system $\dot{u} = \Delta\, \Phi'(u)$ is well defined in the state $u(t_1^*) \in \partial X_1 \cap \partial X_2$ and points *into* X_2, where ∂X_k denotes the topological boundary of X_k in $\ell^\infty(\mathbb{Z})$. We therefore find a time $t_* > t_1^*$ such that the local solution to the microscopic dynamics from the first step has unique continuation to the time interval $[0, t_*)$ with $u(t) \in X_2$ for all $t \in (t_1^*, t_*)$. By construction, u_j and $\dot{u}_j$ are continuous at t_1^* for $j \neq 1$, whereas

$$u_1(t_1^*) = \lim_{t \to t_1^*} u_1(t) = 0, \qquad \dot{u}_1(t_1^*) = \lim_{t \searrow t_1^*} \dot{u}_1(t) = 4 + \lim_{t \nearrow t_1^*} \dot{u}_1(t) \geq 4.$$

thanks to $\operatorname{sgn} u_1(t_1^*) = \lim_{t \searrow t_1^*} \operatorname{sgn} u_1(t) = +1$ and $\lim_{t \nearrow t_1^*} u_1(t_1^*) = -1$. Finally, repeating all arguments from the first step we show that this solution in X_2 exists uniquely until a time t_2^* with $t_1^* < t_2^* \leq \infty$ and $u_2(t_2^*) = 0$ in case of $t_2^* < \infty$.

Condition for $u_0(t_1^*)$ and lower bound for $t_2^* - t_1^*$: For $0 < t < t_1^*$ we infer from (3.3) that

$$\dot{u}_1(t) = \big(u_0(t) + u_2(t) - 2u_1(t)\big) - \big((+1) + (-1) - 2(-1)\big) \le u_0(t) + u_2(t) - 2u_1(t) - 2.$$

Passing to the limit $t \nearrow t_1^*$ we therefore get

$$0 \le \dot{u}_1(t_1^*) \le u_0(t_1^*) + u_2(t_1^*) - 2 < u_0(t_1^*) - 2$$

and hence $u_0(t_1^*) > 2$. In the same way we prove $u_1(t_2^*) > 2$ and conclude that the interface can shift from $k = 1$ to $k = 2$ at time t_2^* only if

$$2 < u_1(t_2^*).$$

Moreover, $u(t) \in X_2$ for all $t \in (t_1^*, t_2^*)$ implies

$$\dot{u}_1(t) = \big(u_0(t) + u_2(t) - 2u_1(t)\big) - \big((+1) + (-1) - 2(+1)\big) \le D + 2 - 2u_1(t).$$

By the comparison principle we therefore have

$$u_1(t) \le \Big(1 - e^{-2t+2t_1^*}\Big)\frac{D+2}{2},$$

and setting $t = t_2^*$ we obtain the estimate for $t_2^* - t_1^*$.

Final step: All arguments derived above can easily be iterated, so the assertions of Theorem 3.2 are proved by induction. In particular, the lower bound for $t_{k+1}^* - t_k^*$ ensures that the solution exists for *all* times $t \ge 0$. □

Remark 3.3. Theorem 3.2 can be adapted to finite lattice systems with $j = 1, \dots, M$ provided that the corresponding ODE system is closed by imposing

1. either *homogeneous Neumann boundary conditions* via $u_0(t) = u_1(t)$ and $u_{M+1}(t) = u_M(t)$,
2. or *inhomogeneous Dirichlet boundary conditions* via $u_0(t) \equiv c_1 > 0$ and $u_{M+1}(t) \equiv c_2 < 0$,

where $j = 0$ and $j = M + 1$ are the ghost indices.

The proof of Theorem 3.2 reveals that the condition $\operatorname{sgn} 0 = 1$ (or equivalently, the right-sided continuity of Φ') is crucial for the microscopic dynamics to be well defined after the phase transition time t_k^* as it guarantees that $u_k(t_k^*) = 0$ implies the *strict* inequality $\dot{u}_k(t_k^* + 0) > 0$. Our convention (3.2) is therefore implicitly but intimately related to phase interfaces that propagate *into* the phase $u < 0$ (to observe phase propagation into to the other phase $u > 0$, one has to set $\operatorname{sgn} 0 = -1$). This subtle direction selection reflects that the spinodal region is actually an isolated point and can be regarded as the degenerate analogue to the hysteresis flow rule (1.10).

Corollary 3.4 (criterion for standing interfaces)**.** *For single-interface initial data*

$$u(0) \in X_{k_1} \qquad \textit{with} \qquad \sup_{j \in \mathbb{Z}} u_j(0) \le 2$$

we find $t_{k_1}^* = \infty$ and hence a standing-interface solution.

We finally characterize the evolution of $p_j(t) = \Phi'(u_j(t))$ for single-interface solutions. The key observations are as follows:

1. p solves the linear discrete heat equation $\dot{p} = \Delta p$ on each time interval (t_k^*, t_{k+1}^*) because $u(t) \in X_k$ implies $p_j(t) = u_j(t) + \operatorname{sgn}(j - k)$ and hence $\dot{p}_j(t) = \dot{u}_j(t)$.
2. At each phase transition time $t_k^* < \infty$, the value of p_k jumps down according to

$$\lim_{t \nearrow t_k^*} p_k(t) = +1, \qquad \lim_{t \searrow t_k^*} p_k(t) = -1$$

but we have $\lim_{t \nearrow t_k^*} p_j(t) = \lim_{t \searrow t_k^*} p_j(t)$ for all $j \ne k$.

The dynamics of p can therefore be interpreted as solving the linear discrete heat equation for $t \geq 0$ where at each phase transition time t_k^* we perturb the system by adding $-2\delta_j^k$ to the current state. Combining this interpretation with the superposition principle we conclude that p consists of a *regular* part q and a *singular* part r, which account for effects of the initial data and the perturbations induced by the phase transitions, respectively. In particular, denoting by g the discrete heat kernel, that is

$$\begin{aligned} \dot{g}_j(t) &= \Delta\, g_j(t), \\ g_j(0) &= \delta_j^0, \end{aligned} \tag{3.4}$$

we arrive at the following result, see also Figure 3.2.

Corollary 3.5 (decomposition of p)**.** *For each single-interface solution we have*

$$p_j(t) = q_j(t) + r_j(t),$$

with

$$r_j(t) := -2 \sum_{k \geq k_1} \chi_{\{t \geq t_k^*\}}(t) g_{j-k}(t - t_k^*),$$

where q is the solution of the discrete heat equation with initial data $q_j(0) = p_j(0)$ and χ_J denotes the indicator function of the set J.

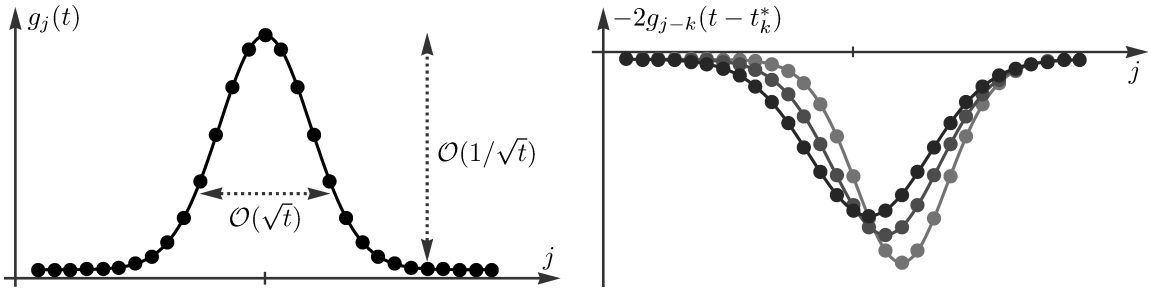

Figure 3.2: *Left.* Cartoon of the discrete heat kernel g (the thin lines represent interpolating splines and are drawn for better illustration). *Right.* The lattice function r is at any time t given by a finite sum of shifted and delayed version of the discrete heat kernel.

The decomposition formula from Corollary 3.5 is crucial for our analysis. In particular, the decay and continuity properties of the discrete heat kernel, see appendix A, enable us to estimate the impact of the sequence of singularities induced by the phase transitions. Notice however, that the evolution of p is still nonlinear as the phase transition times t_k^* depend on p itself.

3.2 Upper bounds for the macroscopic interface speed

In Theorem 3.2 we have shown that single-interface solutions exist. In order to pass to the macroscopic limit, we must however guarantee that the corresponding macroscopic interface speed is at most of order $O(1)$. More precisely, for a given macroscopic distance $\delta > 0$ we have to ensure that the macroscopic time $\varepsilon^2 t^*_{\lfloor \delta/\varepsilon \rfloor}$ is bounded from below by some constant independent of ε, where $\lfloor x \rfloor$ is shorthand for the integer part of x. The derivation of this lower bound is actually at the heart of our convergence proof and requires a careful quantitative analysis of the lattice dynamics. In this paper we restrict ourselves to the most simple case and suppose that the initial data are compatible with the macroscopic limit model. We also assume without loss of generality that the macroscopic interface is initially located at $\xi = 0$.

Assumption 3.6 (macroscopic single-interface initial data)**.** The initial data $u(0)$ belong to X_1 and $p(0) = \Phi'(u(0))$ satisfies

$$|\Delta\, p_0(0)| \leq \beta\varepsilon, \qquad \sup_{j \in \mathbb{Z}} |\nabla_+ p_j(0)| \leq \alpha\varepsilon, \qquad \sup_{j \neq 0} |\Delta\, p_j(0)| \leq \alpha\varepsilon^2.$$

for two constants α and β independent of ε.

Assumption 3.6 is motivated by the limit dynamics, see also Figure 3.3 for an illustration. In fact, the prototypical example for macroscopic single-interface data is

$$p_j(t) = P_{\mathrm{ini}}(\varepsilon j) + c_\varepsilon, \qquad u_j(0) = p_j(t) + \operatorname{sgn}(-j) \tag{3.5}$$

where c_ε is a constant and P_{ini} some given macroscopic function independent of ε such that:

1. P_{ini} is bounded and continuous for all $\xi \in \mathbb{R}$ with

$$P_{\mathrm{ini}}(\xi) > 1 \quad \text{for} \quad \xi < 0 \qquad \text{and} \qquad -1 < P_{\mathrm{ini}}(\xi) < 1 \quad \text{for} \quad \xi > 0$$

and

$$\liminf_{\xi \to -\infty} P_{\mathrm{ini}}(\xi) > 1 \qquad \text{and} \qquad -1 < \liminf_{\xi \to +\infty} P_{\mathrm{ini}}(\xi) \leq \limsup_{\xi \to +\infty} P_{\mathrm{ini}}(\xi) < +1.$$

2. P_{ini} is twice continuously differentiable for $\xi < 0$ and $\xi > 0$ with

$$\beta := \lim_{\xi \searrow 0} \left| P'_{\mathrm{ini}}(+\xi) - P'_{\mathrm{ini}}(-\xi) \right| < \infty, \qquad \alpha := \sup_{\xi \neq 0} \left| P'_{\mathrm{ini}}(\xi) \right| + \left| P''_{\mathrm{ini}}(\xi) \right| < \infty,$$

3. $c_\varepsilon > 0$ is sufficiently small with $c_\varepsilon \to 0$ as $\varepsilon \to 0$ and chosen such that $t_1^* > 0$, that means $u_j(0) > 0$ for all $j \leq 0$ and $u_j(0) < 0$ for all $j \geq 1$.

Corollary 3.7 (bounds for the regular part q)**.** *We have*

$$|\nabla_+ q_j(t)| \leq \alpha\varepsilon \qquad \textit{and} \qquad |\dot{q}_j(t)| = |\Delta\, q_j(t)| \leq \alpha\varepsilon^2 + \beta\varepsilon g_0(t)$$

for all $t \geq 0$, $j \in \mathbb{Z}$, and $\varepsilon > 0$.

Proof. By construction and Assumption 3.6 we have

$$\tfrac{\mathrm{d}}{\mathrm{d}t}\dot{q}_j(t) = \Delta\, \dot{q}_j(t), \qquad |\dot{q}_j(0)| = |\dot{p}_j(0)| = |\dot{u}_j(0)| = |\Delta\, p_j(0)| \leq \alpha\varepsilon^2 + \beta\varepsilon\delta_j^0$$

as well as

$$\tfrac{\mathrm{d}}{\mathrm{d}t}\nabla_+ q_j(t) = \Delta\, \nabla_+ q_j(t), \qquad |\nabla_+ q_j(0)| = |\nabla_+ p_j(0)| \leq \alpha\varepsilon.$$

The claim now follows using both the superposition and the maximum principle for the discrete heat equation. □

We remark that the assertions of Corollary 3.7 are sufficient for showing that the macroscopic interface speed is bounded. All results derived below therefore hold (with different constants) even in the case that

1. $|\nabla_+ p_j(0)| \leq \alpha\varepsilon$ and $|\Delta\, p_j(0)| \leq \beta\varepsilon$ for all $j \in \mathbb{Z}$,
2. $|\Delta\, p_j(0)| \leq \alpha\varepsilon^2$ for almost all $j \in \mathbb{Z}$,

that means the derivative of the function P_{ini} from (3.5) can even be discontinuous at finitely many points.

We are now able to derive upper bounds for the macroscopic interface speed. To this end we prove that Assumption 3.6 implies that the time $t_{k+1}^* - t_k^*$ between two adjacent phase transitions is mesoscopic as it can be bounded from below by $1/\varepsilon$ (recall that Theorem 3.2 provides only $t_{k+1}^* - t_k^* \geq 2/(D-2)$). Our considerations are based on the estimate

$$2 \leq p_k\big(t_{k+1}^*\big) - p_k(t_k^*) = \int_{t_k^*}^{t_{k+1}^*} \dot{p}_k(t)\,\mathrm{d}t = \int_{t_k^*}^{t_{k+1}^*} \dot{q}_k(t)\,\mathrm{d}t - 2\sum_{n=1}^{k} \int_{t_k^*}^{t_{k+1}^*} \dot{g}_{k-n}(t - t_n^*)\,\mathrm{d}t, \tag{3.6}$$

which follows from combining the conditions $u_k(t_k^*) = 0$ and $u_k(t_{k+1}^*) \geq 2$ with the representation formula from Corollary 3.5.

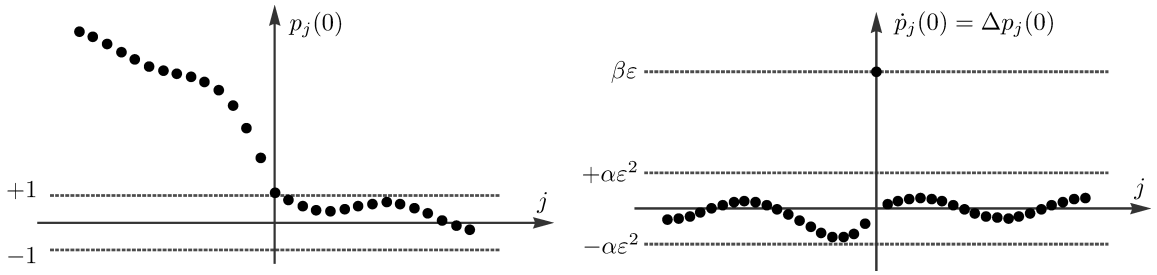

Figure 3.3: For initial data as in Assumption 3.6, the discrete data $p_j(0)$ resemble a macroscopic function P_{ini} that is continuous and piecewise twice continuously differentiable. In particular, the initial velocities $\dot u_j(0) = \dot p_j(0)$ satisfy $\dot p_0(0) = \beta\varepsilon$ and $|\dot p_j(0)| \le \alpha\varepsilon^2$ for $j \neq 0$.

Lemma 3.8 (refined lower bound for the time between two phase transitions)**.** *For any $\tau_{\mathrm{fin}} > 0$ there is a constant $d_* > 0$, which depends on α, β, and τ_{fin}, along with a constant $0 < \varepsilon_* < 1$, which depends only on α and β, such that*

$$\varepsilon\big(t_{k+1}^* - t_k^*\big) \ge 2d_*$$

holds for all $k \ge 1$ with $0 \le t_k^* \le \tau_{\mathrm{fin}}/\varepsilon^2$ provided that $\varepsilon \le \varepsilon_*$.

Proof. In what follows we consider $k \ge 1$ with $t_k^* < \tau_{\mathrm{fin}}/\varepsilon^2$ and denote by c and C generic constants independent of α, β, and ε.

Weaker variant of (3.6): In order to study the implications of (3.6), we first simplify the right hand side as follows. By Lemma A.2 we have

$$-\sum_{n=1}^{k}\int_{t_k^*}^{t_{k+1}^*} \dot g_{k-n}(t - t_n^*)\,\mathrm{d}t \le -\sum_{n=1}^{k}\int_{t_k^*}^{t_{k+1}^*} \dot g_0(t - t_n^*)\,\mathrm{d}t = \sum_{n=1}^{k} g_0(t_k^* - t_n^*) - \sum_{n=1}^{k} g_0\big(t_{k+1}^* - t_n^*\big).$$

whereas Corollary 3.7 provides

$$\int_{t_k^*}^{t_{k+1}^*} \dot q_k(t)\,\mathrm{d}t \le \int_{t_k^*}^{t_{k+1}^*} \big(\alpha\varepsilon^2 + \beta\varepsilon g_0(t)\big)\,\mathrm{d}t$$

Rearranging terms and using $g_0(0) = 1$, inequality (3.6) becomes

$$\sum_{n=1}^{k} g_0(t_{k+1}^* - t_n^*) \le \frac{1}{2}\int_{t_k^*}^{t_{k+1}^*} \big(\alpha\varepsilon^2 + \beta\varepsilon g_0(t)\big)\,\mathrm{d}t + \sum_{n=1}^{k-1} g_0(t_k^* - t_n^*),$$

and writing $s_k := t_{k+1}^* - t_k^*$ we arrive at

$$\sum_{n=1}^{k} g_0(s_k + \cdots + s_n) \le \frac{1}{2}\int_{t_k^*}^{t_k^*+s_k} \big(\alpha\varepsilon^2 + \beta\varepsilon g_0(t)\big)\,\mathrm{d}t + \sum_{n=1}^{k-1} g_0(s_{k-1} + \cdots + s_n). \tag{3.7}$$

In the remainder of this proof we transform this inequality into a lower bound for s_k.

Estimate for $k = 1$: Inequality (3.7) combined with Lemma A.1 provides

$$g_0(s_1) \le \tfrac{1}{2}\int_{t_1^*}^{t_1^*+s_1} \big(\alpha\varepsilon^2 + \beta\varepsilon g_0(t)\big)\,\mathrm{d}t \le \tfrac{1}{2}\int_{0}^{s_1} \big(\alpha\varepsilon^2 + \beta\varepsilon g_0(t)\big)\,\mathrm{d}t,$$

and we deduce that there exists $\varepsilon_* > 0$, which depends on α and β, such that $s_1 \ge 1$ for all $\varepsilon \le \varepsilon_*$. We employ Lemma A.2 again to estimate

$$\frac{c}{\sqrt{s_1}} \le C\big(\alpha\varepsilon^2 + \beta\varepsilon\sqrt{s_1}\big),$$

and this gives

$$\varepsilon s_1 \ge d_1 > 0$$

for some constant d_1 which depends on α and β but not on ε. For $\beta = 0$ we even find $\varepsilon^{4/3} s_1 \geq d_1$.

Estimate for $k > 1$ in a special case: For the following considerations we further suppose that

$$s_k < \min_{n=1,\dots,k-1} s_n.$$

Since g_0 is strictly decreasing, we therefore get

$$g_0(s_k + \cdots + s_{n+1}) > g_0(s_{k-1} + \cdots + s_n)$$

for all $n = 1, \dots, k-1$, and hence

$$g_0(s_k + \cdots + s_1) < \frac{1}{2} \int_{t_k^*}^{t_k^* + s_k} \big(\alpha\varepsilon^2 + \beta\varepsilon g_0(t)\big)\, \mathrm{d}t,$$

thanks to (3.7). This implies $f_k(s_k) < 0$ for

$$f_k(s) := g_0(s + t_k^*) - \frac{1}{2} \int_{t_k^*}^{t_k^* + s} \big(\alpha\varepsilon^2 + \beta\varepsilon g_0(t)\big)\, \mathrm{d}t,$$

where we used that $g_0(s_k + \cdots + s_1) = g_0(s_k + t_k^* - t_1^*) \geq g_0(s_k + t_k^*)$. The properties of g_0, see Lemma A.1 once more, guarantee that the function f_k is convex, continuous, and strictly decreasing in s. Therefore, and in view of $f_k(0) > 0$ and $\lim_{s\to\infty} f_k(s) = -\infty$, we conclude that f_k has a unique zero $\bar{s}_k$ with $\bar{s}_k < s_k$. Due to convexity of f_k we also find

$$\hat{s}_k < \bar{s}_k < s_k,$$

where $\hat{s}_k := -f_k(0)/f_k'(0)$ is the first approximation to $\bar{s}_k$ when starting the Newton algorithm at $s = 0$. By direct computations we now verify

$$\hat{s}_k = \frac{g_0(t_k^*)}{-\dot{g}_0\big(t_k^*\big) + \frac{\alpha\varepsilon^2}{2} + \frac{\beta\varepsilon}{2} g_0(t_k^*)},$$

and using $t_k^* \geq s_1 \geq 1$ as well as Lemma A.2 we obtain

$$\hat{s}_k \geq \frac{c(t_k^*)^{-1/2}}{C\big(t_k^*\big)^{-3/2} + \alpha\varepsilon^2 + C\beta\varepsilon\big(t_k^*\big)^{-1/2}} \geq \frac{c}{\big(t_k^*\big)^{-1} + \alpha\varepsilon^2\big(t_k^*\big)^{1/2} + \beta\varepsilon},$$

and hence

$$\varepsilon s_k \geq \frac{c}{d_1^{-1} + \alpha\tau_{\mathrm{fin}}^{1/2} + \beta} =: d_2$$

where we used that $t_k^* \geq s_1 \geq d_1/\varepsilon$ and $t_k^* \leq \tau_{\mathrm{fin}}/\varepsilon^2$.

Estimate for $k > 1$ in the general case: We have established the estimate $\varepsilon s_1 \geq d_1$ as well as the implication

$$\varepsilon s_k \leq \min\{\varepsilon s_1, \dots, \varepsilon s_{k-1}\} \quad \Longrightarrow \quad \varepsilon s_k \geq d_2,$$

and the desired estimate for s_k follows with $d_* := \frac{1}{2}\min\{d_1, d_2\}$ by induction. □

From Lemma 3.8 we immediately obtain $t_k^* \geq 2kd_*/\varepsilon$ and we deduce for each macroscopic time τ_{fin} that at most $\tau_{\mathrm{fin}}/(2\varepsilon d_*)$ phase transitions can happen for $\tau \leq \tau_{\mathrm{fin}}$, shifting the interface over a macroscopic distance smaller than $\tau_{\mathrm{fin}}/(2d_*)$.

We conclude this section with some comments concerning the microscopic fluctuations caused by the phase transition of u_k at t_k^*. The properties of the discrete heat kernel imply that the amplitude as well the inverse length of the effective spatial support scale with

$$\frac{\varepsilon}{\sqrt{\varepsilon^2 + \big(\tau - \varepsilon^2 t_k^*\big)}},$$

which decays quite rapidly within a macroscopic time of order ε^2 but much slower afterwards. In particular, when u_{k+1} undergoes the next phase transition at time t^*_{k+1}, the fluctuations evoked by u_k have reached an amplitude of order $\varepsilon^{1/2}$ and spread over a macroscopic length of order $\varepsilon^{-1/2}$. Similarly, the amplitude of the velocity fluctuations at time t^*_{k+1} is of order $\varepsilon^{3/2}$.

These scaling arguments, especially the fractional powers of ε, reveal that *macroscopic* single-interface data are *not* invariant under the dynamics. In other words, the lattice data at times $t \lessapprox t^*_k$ – this means just before the phase transitions – do *not* satisfy Assumption 3.6, and we conclude that interface propagation in discrete forward-backward diffusion equations is not only a two-scale but a genuine multi-scale problem.

3.3 Macroscopic continuity and compactness results

In order to pass to the macroscopic limit $\varepsilon \to 0$, we regard the discrete data $p_j(t)$, $q_j(t)$, and $r_j(t)$ as piecewise constant functions with respect to the macroscopic coordinates (τ, ξ). More precisely, we set

$$P_\varepsilon\big(\tau,\, \xi + \zeta\big) := p_{\xi/\varepsilon}\big(\tau/\varepsilon^2\big) \qquad \text{for all} \quad \tau \geq 0, \quad \xi \in \varepsilon\mathbb{Z}, \quad \zeta \in [-\varepsilon/2, +\varepsilon/2)$$

and define Q_ε and R_ε by analogous formulas. We further introduce the macroscopic interface position

$$\xi^*_\varepsilon(\tau) := \varepsilon \sum_{k=1}^{\infty} k \chi_{[t^*_k, t^*_{k+1})}\big(\tau/\varepsilon^2\big) \qquad \text{for all} \quad \tau \geq 0,$$

as a piecewise constant function in time that jumps at the macroscopic phase transitions times defined by

$$\tau^*_{k,\,\varepsilon} := \varepsilon^2 t^*_k \qquad \text{for all} \quad k \in \mathbb{Z}.$$

In what follows we fix a macroscopic final time $0 < \tau_{\text{fin}} < \infty$ and wish to pass to the limit $\varepsilon \to 0$ on the macroscopic time-space domain

$$\Omega := I \times \mathbb{R}, \qquad I := [0, \tau_{\text{fin}}].$$

To this end, we recall that Lemma 3.8 provides constants $d_* > 0$ and $0 < \varepsilon_* \leq 1$ such that

$$K_\varepsilon \leq \frac{\tau_{\text{fin}}}{2d_*\varepsilon}, \qquad \inf_{k=1,\dots,K_\varepsilon} \tau^*_{k+1,\,\varepsilon} - \tau^*_{k,\,\varepsilon} \geq 2d_*\varepsilon \tag{3.8}$$

holds for all $0 < \varepsilon \leq \varepsilon_*$, where

$$K_\varepsilon := \max\Big\{k \in \mathbb{Z} \;:\; \tau^*_{k,\,\varepsilon} < \tau_{\text{fin}}\Big\}$$

is the number phase transitions taking place in the microscopic time interval $[0, \tau_{\text{fin}}/\varepsilon^2]$. Notice that d_*, ε_*, and all constants derived below depend on τ_{fin} and on the initial data via α and β.

Our first result in this section concerns the compactness of the discrete interface curves ξ^*_ε.

Lemma 3.9 (compactness of interface curves)**.** *The family $(\xi_*)_{0<\varepsilon\leq\varepsilon_*}$ is compact in $\mathsf{L}^\infty(I)$ and each limit curve is Lipschitz continuous.*

Proof. We define a piecewise linear function $\bar\xi^*_\varepsilon$ on $[0, \tau_{\text{fin}}]$ by the condition

$$\bar\xi^*_\varepsilon\big(\tau^*_{k,\,\varepsilon}\big) = \xi^*_\varepsilon\big(\tau^*_{k,\,\varepsilon}\big)$$

for all $k = 1, \dots, K_\varepsilon$ and $\bar\xi^*_\varepsilon(\tau_{\text{fin}}) = \xi^*_\varepsilon(\tau^*_{K_\varepsilon,\,\varepsilon})$. We readily check that

$$\big|\bar\xi^*_\varepsilon(\tau) - \xi^*_\varepsilon(\tau)\big| \leq \varepsilon, \qquad 0 \leq \tfrac{\mathrm{d}}{\mathrm{d}\tau}\bar\xi^*_\varepsilon(\tau) \leq \frac{\varepsilon}{2d_*\varepsilon}$$

for almost all $\tau \in [0, \tau_{\text{fin}}]$, and conclude that the family $\big(\bar\xi^*_\varepsilon\big)_{0<\varepsilon\leq\varepsilon_*}$ is bounded in $\mathsf{C}^{0,1}(I)$. All claims hence follow from standard results in real analysis. □

Our main goal this section is to derive compactness result for R_ε and Q_ε that imply (i) the existence of pointwise convergent subsequences, and (ii) the continuity of any limit function. In a preparatory step we next derive an auxiliary result for piecewise constant functions F_ε on Ω revealing that for L^∞-compactness it is sufficient to establish uniform Hölder estimates with respect to $\tau \in I$ and discrete $\xi \in \varepsilon\mathbb{Z}$. Here piecewise constant means, as above, continuous with respect to τ but spatially constant in each interval $\xi \in [\varepsilon j - \varepsilon/2,\, \varepsilon j + \varepsilon/2)$, $j \in \mathbb{Z}$. Our auxiliary result and its proof are straight forward and can very likely be found somewhere in the literature on numerical analysis (though we are not aware of any reference).

Lemma 3.10 (compactness criterion for piecewise constant functions)**.** *Let $(F_\varepsilon)_{0<\varepsilon\le\varepsilon_*}$ be a family of bounded and piecewise constant functions on Ω, and suppose that there exist constants $\gamma_1, \gamma_2 \in (0,1]$ and $C > 0$ such that*

$$\big|F_\varepsilon(\tau_2,\, \xi_2) - F_\varepsilon(\tau_1,\, \xi_1)\big| \le C\big(\big|\tau_2 - \tau_1\big|^{\gamma_1} + \big|\xi_2 - \xi_1\big|^{\gamma_2}\big)$$

holds for all $0 < \varepsilon \le \varepsilon_*$, every $\tau_1, \tau_2 \in I$, and all $\xi_1, \xi_2 \in \varepsilon\mathbb{Z}$. Then this family is compact in $\mathsf{L}^\infty(\Omega)$ and any limit function is locally Hölder continuous with exponent $\min\{\gamma_1, \gamma_2\}$.

Proof. For each ε we define a piecewise linear function $\bar F_\varepsilon$ by

$$\bar F_\varepsilon\big(\tau,\, \bar\xi\big) = F_\varepsilon\big(\tau,\, \bar\xi\big) \qquad \text{for all} \quad \tau \in I, \quad \bar\xi \in \varepsilon\mathbb{Z},$$

and our assumptions yield the Hölder continuity of $\bar F_\varepsilon$ with respect to time, that means

$$\big|\bar F_\varepsilon(\tau_2,\, \xi) - \bar F_\varepsilon(\tau_1,\, \xi)\big| \le C\,|\tau_2 - \tau_1|^{\gamma_1}$$

for all $\xi \in \mathbb{R}$ and $\tau_1, \tau_2 \in I$. Moreover, since $\bar F_\varepsilon$ is piecewise linear with respect to ξ and due to

$$\big|F_\varepsilon\big(\tau,\, \bar\xi\big)\big| \le C, \qquad \left|\frac{F_\varepsilon\big(\tau,\, \bar\xi \pm \varepsilon\big) - F_\varepsilon\big(\tau,\, \bar\xi\big)}{\varepsilon}\right| \le C\varepsilon^{\gamma_2 - 1}$$

we verify – discussing the cases $\operatorname{sgn}\zeta_1 = \operatorname{sgn}\zeta_2$ and $\operatorname{sgn}\zeta_1 \ne \operatorname{sgn}\zeta_2$ separately – the estimate

$$\big|\bar F_\varepsilon\big(\tau,\, \bar\xi + \zeta_2\big) - \bar F_\varepsilon\big(\tau,\, \bar\xi + \zeta_1\big)\big| \le C\varepsilon^{\gamma_2 - 1}\,|\zeta_2 - \zeta_1| \le C\,|\zeta_2 - \zeta_1|^{\gamma_2} \tag{3.9}$$

for all $\tau \in I$, $\bar\xi \in \varepsilon\mathbb{Z}$, and all $\zeta_1, \zeta_2 \in [-\varepsilon, +\varepsilon]$. In particular, setting $\zeta_1 = 0$ and taking the supremum over $\bar\xi$ and ζ_2 we obtain the convergence estimate

$$\|F_\varepsilon - \bar F_\varepsilon\|_{\mathsf{L}^\infty(\Omega)} \le C\varepsilon^{\gamma_2}.$$

We next show that $\bar F_\varepsilon$ is Hölder continuous with respect to ξ. To this end, let $\tau \in I$ and $\xi_1, \xi_2 \in \mathbb{R}$ be given and denote by $\bar\xi_i$ the natural projection of ξ_i to $\varepsilon\mathbb{Z}$, that means $\big|\bar\xi_i - \xi_i\big| \le \varepsilon/2$. For $|\xi_1 - \xi_2| \le \varepsilon/2$ we have $\xi_1, \xi_2 \in [\bar\xi_1 - \varepsilon, \bar\xi_1 + \varepsilon]$ and are hence done by (3.9). In the case of $|\xi_2 - \xi_1| > \varepsilon/2$ we combine our assumptions of F_ε with (3.9) and the triangle inequality to obtain

$$\begin{aligned}\big|\bar F_\varepsilon(\tau,\, \xi_2) - \bar F_\varepsilon(\tau,\, \xi_1)\big| &\le C\,\big|\bar\xi_2 - \bar\xi_1\big|^{\gamma_2} + C\varepsilon^{\gamma_2 - 1}\big(\,\big|\xi_1 - \bar\xi_1\big|^{\gamma_2} + \big|\xi_2 - \bar\xi_2\big|^{\gamma_2}\,\big)\\ &\le C\,\big|\bar\xi_2 - \bar\xi_1\big|^{\gamma_2} + C\varepsilon^{\gamma_2}\end{aligned}$$

and the desired estimate follows with

$$\big|\bar\xi_1 - \bar\xi_2\big| \le |\xi_2 - \xi_1| + 2\cdot\varepsilon/2 \le 3\,|\xi_2 - \xi_1|\,.$$

The claim of the Lemma is now a consequence of the convergence estimate, the spatial and temporal Hölder estimates for $\bar F_\varepsilon$, and the Arzelá-Ascoli theorem applied to $\bar F_\varepsilon$. □

Since the functions Q_ε are obtained by solving the discrete heat equation with macroscopic initial data, they converge as $\varepsilon \to 0$ to a smooth solution of the macroscopic heat equation $\partial_\tau Q = \partial_\xi^2 Q$. This is not surprising and can be proven in many different ways. For our purposes, it is sufficient to observe that strong compactness is provided by combining Lemma 3.10 with the following Hölder estimates.

Lemma 3.11 (Hölder estimates for Q_ε)**.** *There exists a constant C independent of ε such that*

$$\big|Q_\varepsilon(\tau_2,\,\xi_2)-Q_\varepsilon(\tau_1,\,\xi_1)\big|\le C\big(\,|\tau_2-\tau_1|^{1/2}+|\xi_2-\xi_1|\,\big)$$

holds with $\xi_1,\xi_2\in\varepsilon\mathbb{Z}$ and $0\le\tau_1,\tau_2\le\tau_{\mathrm{fin}}$ for all $0<\varepsilon\le\varepsilon_*$.

Proof. From Corollary 3.7 and $|g_0(t)|\le Ct^{-1/2}$ we derive

$$|q_j(t_2)-q_j(t_1)|\le\int_{t_1}^{t_2}|\dot q_j(t)|\,\mathrm{d}t\le\alpha\varepsilon^2(t_2-t_1)+C\beta\varepsilon\big(\sqrt{t_2}-\sqrt{t_1}\big),$$

as well as

$$\big|q_{j_2}(t_1)-q_{j_1}(t_1)\big|\le\sum_{j=j_1}^{j_2-1}\big|\nabla_+q_j(t_1)\big|\le\alpha\varepsilon(j_2-j_1)$$

for all $j_1,j_2\in\mathbb{Z}$ with $j_1<j_2$ and all $0\le t_1\le t_2<\infty$. Setting $j_i=\xi_i/\varepsilon$ and $t_i=\tau_i/\varepsilon^2$ we therefore get

$$\big|Q_\varepsilon(\tau_2,\,\xi_2)-Q_\varepsilon(\tau_1,\,\xi_1)\big|\le\alpha(\xi_2-\xi_1)+\alpha(\tau_2-\tau_1)+\beta(\sqrt{\tau_2}-\sqrt{\tau_1}),$$

and the claim follows since $0\le\tau_1\le\tau_2\le\tau_{\mathrm{fin}}$ implies $|\tau_2-\tau_1|+\big(\sqrt{\tau_2}-\sqrt{\tau_1}\big)\le C\sqrt{\tau_2-\tau_1}$. □

A crucial part of our analysis is to establish strong L^∞-compactness of the functions R_ε. The main difficulty is that R_ε equals the sum of K_ε shifted and delayed versions of the discrete heat kernel producing a temporal discontinuity at any of the phase transition times $\tau^*_{1,\,\varepsilon},\dots,\tau^*_{K_\varepsilon,\,\varepsilon}$. In order to control the impact of all these jumps in time we split

$$R_\varepsilon(\tau,\,\xi)=R_{1,\,\varepsilon}(\tau,\,\xi)+R_{2,\,\varepsilon}(\tau,\,\xi)$$

with

$$R_{1,\,\varepsilon}(\tau,\,\xi):=-2\sum_{k=1}^{K_\varepsilon}H_\varepsilon\big(\tau-\tau^*_{k,\,\varepsilon},\,\xi-\varepsilon k\big)$$

and $R_{2,\,\varepsilon}:=R_\varepsilon-R_{1,\,\varepsilon}$. Here the function $H_\varepsilon:\mathbb{R}^2\to\mathbb{R}$,

$$H_\varepsilon(\tau,\,\xi):=\begin{cases}0 & \text{for}\quad\tau\le0,\\ \dfrac{\tau}{d_*\varepsilon}G_\varepsilon(d_*\varepsilon,\,\xi) & \text{for}\quad0\le\tau\le d_*\varepsilon,\\ G_\varepsilon(\tau,\,\xi) & \text{for}\quad\tau\ge d_*\varepsilon\end{cases}$$

can be regarded as a temporally regularized version of G_ε, where the latter represents the discrete heat kernel in macroscopic coordinates according to $G_\varepsilon\big(\varepsilon^2t,\,\varepsilon j\big)=g_j(t)$. In particular, H_ε is continuous with respect to $\tau\in\mathbb{R}$ and differs from G_ε for $0\le\tau\le d_*\varepsilon$ only.

The function $R_{2,\,\varepsilon}$ contains all the temporal jumps caused by the phase transitions and can therefore not be compact $\mathsf{L}^\infty(\Omega)$. The key observation, however, is that $R_{2,\,\varepsilon}$ is still uniformly bounded and converges as $\varepsilon\to0$ to 0 in $\mathsf{L}^s(\Omega)$ for any $1\le s<\infty$. The macroscopic limit of $(R_\varepsilon)_{0<\varepsilon\le\varepsilon_*}$ is therefore completely determined by the family $(R_{1,\,\varepsilon})_{0<\varepsilon\le\varepsilon_*}$, where each function $R_{1,\,\varepsilon}$ is continuous with respect to τ and satisfies

$$Q_\varepsilon\big(\tau^*_{k,\,\varepsilon},\,\varepsilon k\big)+R_{1,\,\varepsilon}\big(\tau^*_{k,\,\varepsilon},\,\varepsilon k\big)=\lim_{\tau\nearrow\tau^*_{k,\,\varepsilon}}P_\varepsilon(\tau,\,\varepsilon k)=1\tag{3.10}$$

for all $k\ge1$ with $\tau^*_{k,\,\varepsilon}\le\tau_{\mathrm{fin}}$ thanks to $\lim_{t\nearrow t^*_k}p_k(t)=1$.

Lemma 3.12 (bounds for $R_{2,\varepsilon}$)**.** *There exists a constant C independent of ε such that*

$$\|R_{2,\varepsilon}\|_{\mathsf{L}^\infty(\Omega)} \le C, \qquad \|R_{2,\varepsilon}\|_{\mathsf{L}^1(\Omega)} \le C\varepsilon$$

holds for all $0 < \varepsilon \le \varepsilon_*$.

Proof. By construction and Corollary 3.5 we have

$$\operatorname{supp} R_{2,\varepsilon} \subset \big(I_{1,\varepsilon} \cup \cdots \cup I_{K_\varepsilon,\varepsilon}\big) \times \mathbb{R}, \qquad I_{k,\varepsilon} := [\tau^*_{k,\varepsilon},\, \tau^*_{k,\varepsilon} + d_*\varepsilon],$$

and the intervals $I_{k,\varepsilon}$ are pairwise disjoint thanks to (3.8). In particular, using

$$R_{2,\varepsilon}\big(\tau^*_{k,\varepsilon} + \sigma,\, j\varepsilon\big) = 2H_\varepsilon(\sigma,\, \varepsilon j - \varepsilon k) - 2G_\varepsilon(\sigma,\, \varepsilon j - \varepsilon k) \qquad \text{for all} \quad j \in \mathbb{Z}, \quad \sigma \le d_*\varepsilon,$$

we estimate

$$\big|R_{2,\varepsilon}\big(\tau^*_{k,\varepsilon} + \sigma,\, j\varepsilon\big)\big| \le 2\Big(G_\varepsilon(0,\, \varepsilon j - \varepsilon k) + G_\varepsilon(d_*\varepsilon,\, \varepsilon j - \varepsilon k)\Big) \le 2,$$

see Lemma A.2, as well as

$$\int_{\mathbb{R}} \big|R_{2,\varepsilon}\big(\tau^*_{k,\varepsilon} + \sigma,\, \xi\big)\big|\, \mathrm{d}\xi \le 2\varepsilon \sum_{j\in\mathbb{Z}} \Big(g_{j-k}(0) + g_{j-k}\big(d_*/\varepsilon\big)\Big) = 4\varepsilon$$

thanks to $\sum_{j\in\mathbb{Z}} g_j(t) = 1$ for all t. The first estimate implies $\|R_{2,\varepsilon}\|_{\mathsf{L}^\infty(\Omega)} \le 2$, whereas the second gives rise to

$$\|R_{2,\varepsilon}\|_{\mathsf{L}^1(\Omega)} \le \sum_{k=1}^{K_\varepsilon} \int_0^{d_*\varepsilon} \int_{\mathbb{R}} \big|R_{2,\varepsilon}\big(\tau^*_{k,\varepsilon} + \sigma,\, \xi\big)\big|\, \mathrm{d}\xi\, \mathrm{d}\sigma \le 2K_\varepsilon d_*\varepsilon^2 \le \tau_{\mathrm{fin}}\varepsilon,$$

where we used (3.8) again. □

It remains to establish L^∞-compactness results for $R_{1,\varepsilon}$. To this end we next derive a further auxiliary result concerning the Hölder continuity of H_ε.

Lemma 3.13 (Hölder estimates for H_ε)**.** *For each $0 < \gamma < 1$ there exists a constant C independent of ε such that*

$$\big|H_\varepsilon(\tau_2,\, \xi_2) - H_\varepsilon(\tau_1,\, \xi_1)\big| \le C\varepsilon\left(\frac{|\tau_2 - \tau_1|^\gamma}{\max\{d_*\varepsilon, \tau_1\}^{\gamma+1/2}} + \frac{|\xi_2 - \xi_1|^{1/2}}{\max\{d_*\varepsilon, \tau_1\}^{3/4}}\right)$$

holds with $\xi_1, \xi_2 \in \varepsilon\mathbb{Z}$ and $0 \le \tau_1 \le \tau_2 \le \tau_{\mathrm{fin}}$ for all $0 < \varepsilon \le \varepsilon_*$.

Proof. Suppose at first that $d_*\varepsilon \le \tau_1 \le \tau_2$. Thanks to the temporal Hölder estimates for the discrete heat kernel, see Lemma A.3, we find

$$\big|H_\varepsilon(\tau_2,\, \xi_2) - H_\varepsilon(\tau_1,\, \xi_2)\big| \le \frac{C\Big(\frac{\tau_2}{\varepsilon^2} - \frac{\tau_1}{\varepsilon^2}\Big)^\gamma}{\Big(\frac{\tau_1}{\varepsilon^2}\Big)^{\gamma+1/2}} = \frac{C\varepsilon}{\tau_1^{\gamma+1/2}}\, |\tau_2 - \tau_1|^\gamma$$

for some constant C independent of ε and ξ_2. Similarly, Lemma A.3 also ensures that

$$\big|H_\varepsilon(\tau_1,\, \xi_2) - H_\varepsilon(\tau_1,\, \xi_1)\big| \le \frac{C\left|\frac{\xi_2}{\varepsilon} - \frac{\xi_1}{\varepsilon}\right|^{1/2}}{\Big(\frac{\tau_1}{\varepsilon^2}\Big)^{3/4}} = \frac{C\varepsilon}{\tau_1^{3/4}}\, |\xi_2 - \xi_1|^{1/2}\,.$$

Now suppose that $0 \le \tau_1 \le \tau_2 \le d_*\varepsilon$. We then estimate

$$\begin{aligned}\big|H_\varepsilon(\tau_2,\,\xi_2) - H_\varepsilon(\tau_1,\,\xi_2)\big| &\le \frac{g_{\xi_2/\varepsilon}\big(d_*/\varepsilon\big)}{d_*\varepsilon}(\tau_2-\tau_1) \le \frac{C}{d_*^{3/2}\varepsilon^{1/2}}(\tau_2-\tau_1)\\ &\le \frac{C}{d_*^{3/2}\varepsilon^{1/2}}(d_*\varepsilon)^{1-\gamma}\,|\tau_2-\tau_1|^\gamma \le \frac{C\varepsilon}{(d_*\varepsilon)^{\gamma+1/2}}\,|\tau_2-\tau_1|^\gamma\end{aligned}$$

as well as

$$\big|H_\varepsilon(\tau_1,\,\xi_2) - H_\varepsilon(\tau_1,\,\xi_1)\big| = \frac{\tau_1}{d_*\varepsilon}\big|g_{\xi_2/\varepsilon}(d_*/\varepsilon) - g_{\xi_1/\varepsilon}(d_*/\varepsilon)\big| \le \frac{C\left|\frac{\xi_2}{\varepsilon}-\frac{\xi_1}{\varepsilon}\right|^{1/2}}{\left(\frac{d_*}{\varepsilon}\right)^{3/4}} = \frac{C\varepsilon\,|\xi_2-\xi_1|^{1/2}}{(d_*\varepsilon)^{3/4}}.$$

In summary, we have established the desired estimates in the special cases $0 \le \tau_1 \le \tau_2 \le d_*\varepsilon$ or $d_*\varepsilon \le \tau_1 \le \tau_2$. All other cases can be easily be traced back to these cases using the triangle inequality. □

We are now able to prove our main technical result in this section.

Lemma 3.14 (Hölder estimates for $R_{1,\,\varepsilon}$)**.** *For each $0 < \gamma < 1/2$ there exists a constant C independent of ε such that*

$$\big|R_{1,\,\varepsilon}(\tau_2,\,\xi_2) - R_{1,\,\varepsilon}(\tau_1,\,\xi_1)\big| \le C\big(\,|\tau_2-\tau_1|^\gamma + |\xi_2-\xi_1|^{1/2}\,\big)$$

holds with $\xi_1, \xi_2 \in \varepsilon\mathbb{Z}$ and $0 \le \tau_1 \le \tau_2 \le \tau_{\text{fin}}$ for all $0 < \varepsilon \le \varepsilon_*$.

Proof. It is sufficient to proof the assertions in time and space separately.

Hölder continuity with respect to ξ: Let $0 \le \tau \le \tau_{\text{fin}}$ and $\xi_1, \xi_2 \in \mathbb{R}$ be given. Then there exists $m_\varepsilon \in \mathbb{Z}$ such that

$$\tau^*_{m_\varepsilon,\,\varepsilon} < \tau \le \tau^*_{m_\varepsilon+1,\,\varepsilon}$$

and (3.8) ensure that $\varepsilon m_\varepsilon \le \tau/(2d_*)$ as well as

$$\tau - \tau^*_{k,\,\varepsilon} \ge 2d_*\varepsilon(m_\varepsilon - k) \qquad \text{for all} \quad k = 1, \dots, m_\varepsilon.$$

In particular, we have

$$H_\varepsilon\big(\tau - \tau^*_{k,\,\varepsilon},\,\xi\big) = 0 \qquad \text{for all} \quad k > m_\varepsilon, \quad \xi \in \mathbb{R},$$

so Lemma 3.13 yields

$$\big|R_{1,\,\varepsilon}(\tau,\,\xi_2) - R_{1,\,\varepsilon}(\tau,\,\xi_1)\big| \le 2\sum_{k=1}^{m_\varepsilon}\big|H_\varepsilon\big(\tau-\tau^*_{k,\,\varepsilon},\,\xi_2\big) - H_\varepsilon\big(\tau-\tau^*_{k,\,\varepsilon},\,\xi_1\big)\big| \le CS_\varepsilon\,|\xi_2-\xi_1|^{1/2}$$

with

$$S_\varepsilon := \sum_{k=1}^{m_\varepsilon}\frac{\varepsilon}{\Big(\max\big\{d_*\varepsilon,\,\tau-\tau^*_{k,\,\varepsilon}\big\}\Big)^{3/4}} \le \frac{1}{d_*} + \sum_{k=1}^{m_\varepsilon-1}\frac{\varepsilon}{(2d_*\varepsilon(m_\varepsilon-k))^{3/4}} \le \frac{1}{d_*} + \frac{1}{2d_*}\int_0^\tau \frac{\mathrm{d}\sigma}{\sigma^{3/4}} \le C,$$

where we used the Riemann sum approximation of the integral as well as the monotonicity of the integrand.

Hölder continuity with respect to τ: Now let $\xi \in \mathbb{R}$ and $0 \le \tau_1 < \tau_2 \le \tau_{\text{fin}}$ be fixed, and choose $m_\varepsilon, n_\varepsilon \in \mathbb{Z}$ such that

$$\tau^*_{m_\varepsilon,\,\varepsilon} < \tau_1 \le \tau^*_{m_\varepsilon+1,\,\varepsilon}, \qquad \tau^*_{n_\varepsilon,\,\varepsilon} < \tau_2 \le \tau^*_{n_\varepsilon+1,\,\varepsilon}.$$

This gives

$$\varepsilon m_\varepsilon \le \tau_1/(2d_*), \qquad \varepsilon(n_\varepsilon - m_\varepsilon) \le (\tau_2 - \tau_1)/(2d_*)$$

as well as

$$\big|R_{1,\varepsilon}(\tau_2, \xi) - R_{1,\varepsilon}(\tau_1, \xi)\big| \le 2X_\varepsilon + 2Y_\varepsilon,$$

where

$$X_\varepsilon := \sum_{k=1}^{m_\varepsilon} \big|H_\varepsilon\big(\tau_2 - \tau^*_{k,\varepsilon}, \xi\big) - H_\varepsilon\big(\tau_1 - \tau^*_{k,\varepsilon}, \xi\big)\big|, \qquad Y_\varepsilon := \sum_{k=m_\varepsilon+1}^{n_\varepsilon} \big|H_\varepsilon\big(\tau_2 - \tau^*_{k,\varepsilon}, \xi\big)\big|.$$

Similar to the above, we deduce that

$$X_\varepsilon \le \sum_{k=1}^{m_\varepsilon} \frac{C\varepsilon\,|\tau_2 - \tau_1|^\gamma}{\max\{d_*\varepsilon,\, \tau - \tau^*_{k,\varepsilon}\}^{\gamma+1/2}} \le C\bigg(\frac{1}{d_*} + \frac{1}{2d_*}\int_0^{\tau_1} \frac{\mathrm{d}\sigma}{\sigma^{\gamma+1/2}}\bigg)\,|\tau_2 - \tau_1|^\gamma \le C\,|\tau_2 - \tau_1|^\gamma,$$

whereas Y_ε can be estimated by

$$\begin{aligned} Y_\varepsilon &\le \sum_{k=m_\varepsilon+1}^{n_\varepsilon} G_\varepsilon\big(\tau_2 - \tau^*_{k,\varepsilon}, 0\big) \le \sum_{k=m_\varepsilon+1}^{n_\varepsilon} G_\varepsilon\big(\tau_2 - 2d_*\varepsilon(n_\varepsilon - k), 0\big) \\ &\le \frac{1}{2d_*\varepsilon}\int_{\tau_1}^{\tau_2} G_\varepsilon(\tau_2 - \sigma, 0)\,\mathrm{d}\sigma = \frac{1}{2d_*\varepsilon}\int_0^{\tau_2-\tau_1} G_\varepsilon(\sigma, 0)\,\mathrm{d}\sigma \\ &\le C\int_0^{\tau_2-\tau_1} \frac{\mathrm{d}\sigma}{\sigma^{1/2}} = C\,|\tau_2 - \tau_1|^{1/2} \le C\,|\tau_2 - \tau_1|^\gamma, \end{aligned}$$

see Lemma A.2 and (3.8). □

We conclude this section by showing that both the L^1-norm of $R_{1,\varepsilon}(\tau, \cdot)$ and the L^2-norm of $\nabla_\varepsilon R_{1,\varepsilon}(\tau, \cdot)$ are bounded uniformly with respect to τ and ε, where

$$\nabla_\varepsilon F(\xi) := \frac{F(\xi + \varepsilon) - F(\xi)}{\varepsilon}$$

is the discrete spatial gradient of a function F defined on $\mathbb{R}$.

Lemma 3.15 (Lebesgue bounds for $R_{1,\varepsilon}$ and its discrete gradient)**.** *There exists a constant C such that*

$$\|R_{1,\varepsilon}\|_{\mathsf{L}^\infty(I;\mathsf{L}^1(\mathbb{R}))} + \|\nabla_\varepsilon R_{1,\varepsilon}\|_{\mathsf{L}^\infty(I;\mathsf{L}^2(\mathbb{R}))} \le C$$

holds for all $0 \le \varepsilon \le \varepsilon_*$.

Proof. For $\tau \ge \varepsilon d_*$, the properties of the discrete heat kernel, see Lemma A.2, imply

$$\int_{\mathbb{R}} H_\varepsilon(\tau, \xi)\,\mathrm{d}\xi = \varepsilon\sum_{j\in\mathbb{Z}} g_j\big(\tau/\varepsilon^2\big) = \varepsilon, \qquad \int_{\mathbb{R}} \Big(\nabla_\varepsilon H_\varepsilon(\tau, \xi)\Big)^2\,\mathrm{d}\xi = \varepsilon^{-1}\sum_{j\in\mathbb{Z}} \Big(\nabla_+ g_j\big(\tau/\varepsilon^2\big)\Big)^2 \le \frac{\varepsilon^2 C}{\tau^{3/2}},$$

and combining this with the definition of H_ε for all $\tau \in \mathbb{R}$ we find

$$\|H_\varepsilon(\tau, \cdot)\|_{\mathsf{L}^1(\mathbb{R})} \le \varepsilon, \qquad \|\nabla_\varepsilon H_\varepsilon(\tau, \cdot)\|_{\mathsf{L}^2(\mathbb{R})} \le C\begin{cases} 0 & \text{for } \tau < 0, \\ \varepsilon^{1/4} & \text{for } 0 < \tau < d_*\varepsilon, \\ \varepsilon\tau^{-3/4} & \text{for } \tau > d_*\varepsilon. \end{cases}$$

From the first estimate we infer that

$$\|R_{1,\varepsilon}(\tau, \cdot)\|_{\mathsf{L}^1(\mathbb{R})} \le \varepsilon K_\varepsilon \le \frac{\tau_{\mathrm{fin}}}{2d_*}$$

holds for all $\tau \in I$. We next fix $\tau \in I$ and choose an integer m_ε such that $\tau^*_{m_\varepsilon,\,\varepsilon} < \tau \le \tau^*_{m_\varepsilon+1,\,\varepsilon}$. As in the first part of the proof of Lemma 3.14, we estimate

$$\begin{aligned}\|\nabla_\varepsilon R_{1,\,\varepsilon}(\tau,\,\cdot)\|_{\mathsf{L}^2(\mathbb{R})} &\le \sum_{k=1}^{m_\varepsilon} \|\nabla_\varepsilon H_\varepsilon\big(\tau - \tau^*_{k,\,\varepsilon},\,\cdot\big)\|_{\mathsf{L}^2(\mathbb{R})} \\ &\le C\varepsilon^{1/4} + \sum_{k=1}^{m_\varepsilon-1} \frac{C\varepsilon}{\big(2kd_*\varepsilon(m_\varepsilon-k)\big)^{3/4}} = C\Big(\varepsilon^{1/4}+1\Big),\end{aligned}$$

and the proof is complete. □

3.4 Convergence results and verification of limit dynamics

In view of the compactness results in Lemmas 3.9, 3.11, and 3.14, we may select a subsequence of $\varepsilon \to 0$, which we do not relabel, such that

$$\xi^*_\varepsilon \to \xi^* \text{ in } \mathsf{L}^\infty(I), \qquad Q_\varepsilon \to Q \text{ in } \mathsf{L}^\infty(\Omega), \qquad R_{1,\,\varepsilon} \to R \text{ in } \mathsf{L}^\infty(\Omega). \tag{3.11}$$

As $R_{2,\,\varepsilon} \to 0$ in $\mathsf{L}^s(\Omega)$ for any $1 \le s < \infty$ by Lemma 3.12, we find

$$P_\varepsilon = Q_\varepsilon + R_{1,\,\varepsilon} + R_{2,\,\varepsilon} \to Q + R = P \qquad \text{in } \mathsf{L}^s_{\mathrm{loc}}(\Omega), \tag{3.12}$$

that means, P is the limit of P_ε in $\mathsf{L}^s_{\mathrm{loc}}(\Omega)$ and the limit of $Q_\varepsilon + R_{1,\,\varepsilon}$ in $\mathsf{L}^\infty(\Omega)$. Moreover, convergence of $(Q_\varepsilon)_\varepsilon$ implies convergence of the initial data

$$P_\varepsilon(0,\cdot) = Q_\varepsilon(0,\cdot) \to Q(0,\cdot) = P(0,\cdot) \qquad \text{in } \mathsf{L}^\infty(\mathbb{R}). \tag{3.13}$$

Theorem 3.16 (limit dynamics along subsequences)**.** *Any limit (P, Q, R, ξ^*) satisfies:*

1. *$\Xi^* := \{(\tau, \xi^*(\tau)) : \tau \in I\}$ is a Lipschitz curve in Ω; the functions Q, R, and $P = Q + R$ are bounded and locally Hölder continuous in Ω; furthermore, $R \in \mathsf{L}^\infty(I; \mathsf{L}^1(\mathbb{R}))$ and $\partial_\xi R \in \mathsf{L}^\infty(I; \mathsf{L}^2(\mathbb{R}))$.*
2. *Q is a solution of the heat equation in Ω with initial data $P(0,\cdot)$.*
3. *(P, ξ^*) is a distributional solution of*

$$\partial_\tau P = \partial_\xi^2 P \ \text{ in } \ \Omega \setminus \Xi^*, \qquad [\![P]\!] = 0 \ \text{ and } \ 2\tfrac{\mathrm{d}}{\mathrm{d}\tau}\xi^* = [\![\partial_\xi P]\!] \ \text{ on } \ \Xi^* \tag{3.14}$$

with initial data $(P(0,\cdot), \xi^*(0))$ attained in $\mathsf{L}^\infty(\mathbb{R}) \times \mathbb{R}$. Moreover, we have

$$\begin{aligned} &P(\tau,\xi) \ge -1 \qquad \text{for all } (\tau,\xi) \in \Omega, \\ &P(\tau,\xi) \le 1 \qquad \text{if } \xi \ge \xi^*(\tau), \end{aligned}$$

which implies $P \in [-1, 1]$ on Ξ^*, and the movement of the interface is determined by

$$\begin{aligned} &\tfrac{\mathrm{d}}{\mathrm{d}\tau}\xi^*(\tau) \ge 0 \qquad \text{for almost all } \tau \in I, \\ &\tfrac{\mathrm{d}}{\mathrm{d}\tau}\xi^*(\tau) = 0 \qquad \text{if } P(\tau,\xi^*(\tau)) \ne 1. \end{aligned}$$

Remark 3.17. Being a distributional solution of (3.14) means

$$-\int_0^{\tau_{\mathrm{fin}}} \int_{\mathbb{R}} (P+\mu)\,\partial_\tau\psi \,\mathrm{d}\xi\,\mathrm{d}\tau = \int_0^{\tau_{\mathrm{fin}}} \int_{\mathbb{R}} P\,\partial_\xi^2\psi \,\mathrm{d}\xi\,\mathrm{d}\tau, \qquad \psi \in \mathsf{C}_c^\infty((0,\tau_{\mathrm{fin}}) \times \mathbb{R}), \tag{3.15}$$

where $\mu(\tau,\xi) = \operatorname{sgn}(\xi^*(\tau) - \xi)$. In the following we will use ξ^* and μ interchangeably to represent the solution, whichever is more convenient.

Proof of Theorem 3.16. The continuity properties of ξ^* and Q are immediate consequences of Lemma 3.9 and Lemma 3.11; Lemma 3.9 also yields $\frac{\mathrm{d}}{\mathrm{d}\tau}\xi^* \geq 0$. Hölder continuity of P and the claims for R follow from $P = Q + R$ and the bounds on $R_{1,\varepsilon}$ proved in Lemmas 3.14 and 3.15.

Setting $\mu_\varepsilon(\tau,\xi) = \operatorname{sgn}(\xi_\varepsilon^*(\tau) - \xi) = \operatorname{sgn} U_\varepsilon(\tau,\xi)$, we write the equation for $U_\varepsilon = P_\varepsilon + \mu_\varepsilon$ in distributional form as

$$-\int_0^{\tau_{\mathrm{fin}}} \int_{\mathbb{R}} (P_\varepsilon + \mu_\varepsilon)\, \partial_\tau \psi \,\mathrm{d}\xi\,\mathrm{d}\tau = \int_0^{\tau_{\mathrm{fin}}} \int_{\mathbb{R}} P_\varepsilon\, \Delta_\varepsilon\, \psi \,\mathrm{d}\xi\,\mathrm{d}\tau, \qquad \psi \in \mathsf{C}_c^\infty((0,\tau_{\mathrm{fin}}) \times \mathbb{R})$$

and deduce (3.15) in the limit $\varepsilon \to 0$. Similarly, Q solves the heat equation, and both P and Q attain their initial data in $\mathsf{L}^\infty(\mathbb{R})$ due to (3.13) and continuity of Q.

By construction, the discrete solutions satisfy $P_\varepsilon \geq -1$ in Ω and $P_\varepsilon \leq 1$ in $\{(\tau,\xi) \in \Omega : \xi \geq \xi_\varepsilon^*(\tau)\}$ for all $\varepsilon > 0$, and in the limit $\varepsilon \to 0$ we obtain the corresponding inequalities for P and ξ^*. In particular, we have $P(\tau, \xi^*(\tau)) \in [-1,1]$ for all $\tau \in I$.

It remains to check that $P(\tau,\xi^*(\tau)) < 1$ implies $\frac{\mathrm{d}}{\mathrm{d}\tau}\xi^*(\tau) = 0$. To this end, let $(\bar\tau,\bar\xi) \in \Xi^*$ and $\delta > 0$ be given such that $P(\bar\tau,\bar\xi) = 1 - 2\delta$, and suppose at first that $\bar\xi < \xi^*(\tau_{\mathrm{fin}})$. For any ε choose $\bar\xi_\varepsilon \in \varepsilon\mathbb{Z}$ such that $\bar\xi_\varepsilon \leq \bar\xi \leq \bar\xi_\varepsilon + \varepsilon$ and denote by $\bar\tau_\varepsilon$ the phase transition time corresponding to $\bar\xi_\varepsilon$. See the left panel of Figure 3.4 for an illustration and notice that $\bar\tau_\varepsilon < \tau_{\mathrm{fin}}$ because otherwise the interface position would be maximal via $\bar\xi = \xi^*(\tau_{\mathrm{fin}})$. Hölder continuity of P now implies

$$P(\bar\tau_\varepsilon,\bar\xi_\varepsilon) - 1 + 2\delta \leq |P(\bar\tau_\varepsilon,\bar\xi_\varepsilon) - P(\bar\tau,\bar\xi)| \leq C\big(|\bar\tau_\varepsilon - \bar\tau|^\gamma + \varepsilon^\gamma\big)$$

for some exponent $0 < \gamma < 1$, while uniform convergence of $Q_\varepsilon + R_{1,\varepsilon} \to P$ as $\varepsilon \to 0$ and $(Q_\varepsilon + R_{1,\varepsilon})(\bar\tau_\varepsilon,\bar\xi_\varepsilon) = 1$, see (3.10), yield

$$P(\bar\tau_\varepsilon,\bar\xi_\varepsilon) \geq 1 - o(1)_{\varepsilon\to 0}.$$

We thus find $\delta \leq C|\bar\tau_\varepsilon - \bar\tau|^\gamma$ for all sufficiently small $\varepsilon > 0$ and may select a subsequence of $\varepsilon \to 0$ such that $\bar\tau_\varepsilon \to \bar\tau_0$ and $\bar\tau_0 < \bar\tau$. The uniform convergence $\xi_\varepsilon^* \to \xi^*$ implies

$$\xi^*(\bar\tau_0) = \lim_{\varepsilon\to 0} \xi_\varepsilon^*(\bar\tau_\varepsilon) = \lim_{\varepsilon\to 0} \bar\xi_\varepsilon = \xi^*(\bar\tau),$$

and $\frac{\mathrm{d}}{\mathrm{d}\tau}\xi^* \geq 0$ ensures that ξ^* is constant in $[\bar\tau_0,\bar\tau]$. By a similar argument using $\hat\xi_\varepsilon = \bar\xi_\varepsilon + \varepsilon$ and the corresponding phase transition time $\hat\tau_\varepsilon$ we finally conclude that $\bar\tau$ is a regular point of ξ^* and $\frac{\mathrm{d}}{\mathrm{d}\tau}\xi^*(\bar\tau) = 0$. Moreover, in case of $\bar\tau < \tau_{\mathrm{fin}}$ and $\bar\xi = \xi^*(\tau_{\mathrm{fin}})$ we find that ξ^* is constant on $[\bar\tau,\tau_{\mathrm{fin}}]$, and for $\bar\tau = \tau_{\mathrm{fin}}$ we can repeat the above reasoning after enlarging the time interval slightly beyond τ_{fin}. □

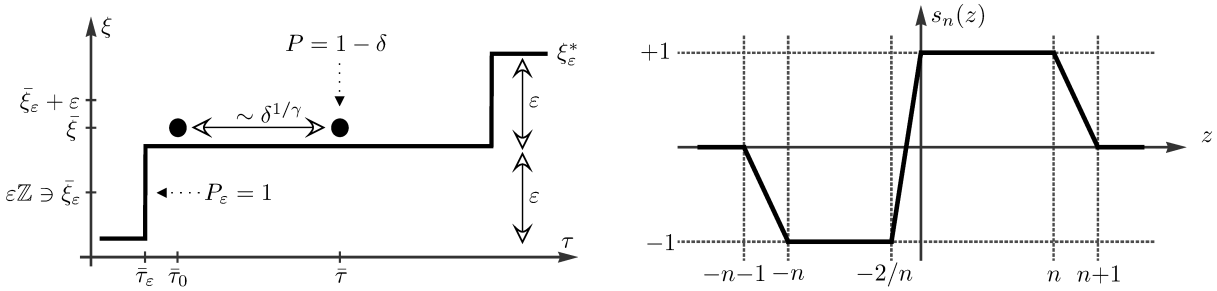

Figure 3.4: *Left.* Illustration of the key argument in the proof of Theorem 3.16: By construction, we have $\bar\xi = \xi^*(\bar\tau) = \xi^*(\bar\tau_0)$ and $\frac{\mathrm{d}}{\mathrm{d}\tau}\xi^* \geq 0$, so ξ^* is constant on $[\bar\tau_0,\bar\tau]$. *Right.* Approximation s_n of the sign function used in the proof of Theorem 3.18 for the case $\xi_1^* \geq \xi_2^*$; for $\xi_1^* \leq \xi_2^*$ one has to redefine s_n such that $s_n(0) = -1$.

We complement Theorem 3.16 with a uniqueness result by adapting some techniques for hysteresis problems from [Hil89, Vis06].

Theorem 3.18 (well-posedness of the limit problem)**.** *The solution to the limit problem in Theorem 3.16 is uniquely determined by the initial data $P(0,\cdot)$ and $\xi^*(0)$.*

Proof. Given two solutions (P_1, Q_1, R_1, ξ_1^*) and (P_2, Q_2, R_2, ξ_2^*) with initial data $P_1(0,\cdot) = P_2(0,\cdot)$ and $\xi_1^*(0) = \xi_2^*(0)$, we set $\overline{P} = P_1 - P_2$ and $\overline{\mu} = \mu_1 - \mu_2$, where $\mu_i(\tau,\xi) = \operatorname{sgn}(\xi_i^*(\tau) - \xi)$ as in Remark 3.17. In order to show $\overline{P} = \overline{\mu} = 0$ we follow the strategy of [Hil89, Theorem 5], that means we first establish sufficient regularity in time and derive afterwards an L^1-contraction inequality by testing the equation for $\overline{P}$ with $\operatorname{sgn}\overline{P}$.

Regularity in time: Standard uniqueness results for the heat equation imply $Q_1 = Q_2$, and we find $\overline{P} = R_1 - R_2 \in \mathsf{L}^\infty(I;\mathsf{L}^1(\mathbb{R}))$ and $\partial_\xi \overline{P} \in \mathsf{L}^\infty(I;\mathsf{L}^2(\mathbb{R}))$ in addition to boundedness and continuity. Furthermore, $\bar\mu(\tau,\xi)$ is bounded, and it is nonzero only if ξ lies between $\xi_1^*(\tau)$ and $\xi_2^*(\tau)$. We thus conclude

$$\overline{P} \in \mathsf{L}^\infty(I;\mathsf{L}^1(\mathbb{R})) \cap \mathsf{L}^\infty(I;\mathsf{H}^1(\mathbb{R})) \qquad \text{and} \qquad \bar\mu \in \mathsf{L}^\infty(I;\mathsf{L}^2(\mathbb{R})). \tag{3.16}$$

In view of (3.16), we may integrate by parts after subtracting the equations for (P_1,μ_1) and (P_2,μ_2) from each other, which gives

$$\int_0^{\tau_{\mathrm{fin}}} \partial_\tau\phi(\tau) \int_{\mathbb{R}} \big(\overline{P} + \bar\mu\big)(\tau,\xi)\,\eta(\xi)\,\mathrm{d}\xi\,\mathrm{d}\tau = \int_0^{\tau_{\mathrm{fin}}} \phi(\tau) \int_{\mathbb{R}} \partial_\xi \overline{P}(\tau,\xi)\,\partial_\xi\eta(\xi)\,\mathrm{d}\xi\,\mathrm{d}\tau$$

for all $\phi \in \mathsf{C}_c^\infty(I)$, $\eta \in \mathsf{C}_c^\infty(\mathbb{R})$, and by density also for all $\phi \in \mathsf{H}_0^1(I)$, $\eta \in \mathsf{H}^1(\mathbb{R})$. Consequently,

$$\frac{\mathrm{d}}{\mathrm{d}\tau} \int_{\mathbb{R}} \big(\overline{P}(\tau,\xi) + \bar\mu(\tau,\xi)\big)\,\eta(\xi)\,\mathrm{d}\xi = -\int_{\mathbb{R}} \partial_\xi \overline{P}(\tau,\xi)\,\partial_\xi\eta(\xi)\,\mathrm{d}\xi \tag{3.17}$$

for all $\tau \in I$. A direct computation shows that

$$\frac{\mathrm{d}}{\mathrm{d}\tau} \int_{\mathbb{R}} \bar\mu(\tau,\xi)\,\eta(\xi)\,\mathrm{d}\xi = 2\eta(\xi_1^*(\tau))\,\tfrac{\mathrm{d}}{\mathrm{d}\tau}\xi_1^*(\tau) - 2\eta(\xi_2^*(\tau))\,\tfrac{\mathrm{d}}{\mathrm{d}\tau}\xi_2^*(\tau) \tag{3.18}$$

for all $\tau \in I$ where $\frac{\mathrm{d}}{\mathrm{d}\tau}\xi_1^*(\tau)$ and $\frac{\mathrm{d}}{\mathrm{d}\tau}\xi_2^*(\tau)$ are defined, and the right hand side of (3.18) can easily be bounded by $C\|\eta\|_{\mathsf{H}^1(\mathbb{R})}$, where the constant C depends on $\|\xi_j^*\|_{\mathsf{W}^{1,\infty}(I)}$, $j = 1, 2$. Thus, $\partial_\tau\overline{P}(\tau,\cdot)$ exists in $\mathsf{H}^1(\mathbb{R})$ and

$$\big|\big\langle \partial_\tau\overline{P}(\tau,\cdot),\eta\big\rangle\big| = \left|\tfrac{\mathrm{d}}{\mathrm{d}\tau}\int_{\mathbb{R}} \overline{P}(\tau,\xi)\,\eta(\xi)\,\mathrm{d}\xi\right| \le C\left(\|\partial_\xi\overline{P}\|_{\mathsf{L}^\infty(I;\mathsf{L}^2(\mathbb{R}))} + 1\right)\|\eta\|_{\mathsf{H}^1(\mathbb{R})}.$$

By standard embedding results, see for instance [Eva98, Thm. 3 in Sec. 5.9] and note that I is bounded, $\partial_\tau\overline{P} \in \mathsf{L}^\infty(I;\mathsf{H}^{-1}(\mathbb{R}))$ and $\overline{P} \in \mathsf{L}^\infty(I;\mathsf{H}^1(\mathbb{R}))$ imply $\overline{P} \in \mathsf{C}(I;L^2(\mathbb{R}))$, and with (3.16) we conclude $\overline{P} \in \mathsf{C}(I;L^1(\mathbb{R}))$.

Contraction inequality: Given $\tau \in [\tau_1,\tau_2]$, where $0 \le \tau_1 < \tau_2 \le \tau_{\mathrm{fin}}$ such that $\xi_1^* \ge \xi_2^*$ in $[\tau_1,\tau_2]$, we approximate the sign function by

$$s_n(z) = \begin{cases} \max(-1,\min(1,1+nz)) & \text{if } |z| \le n,\\ n + \operatorname{sgn} z - |z| & \text{if } n < |z| \le n+1,\\ 0 & \text{otherwise,}\end{cases}$$

see Figure 3.4 for an illustration. In what follows we suppose $n > \|\overline{P}\|_\infty$ and consider $\eta = s_n(\overline{P}(\tau,\cdot)) \in \mathsf{H}^1(\mathbb{R})$ in (3.17)–(3.18). Due to $\overline{P}(\tau,\xi_1^*(\tau)) \ge 0$ if $\frac{\mathrm{d}}{\mathrm{d}\tau}\xi_1^*(\tau) > 0$ and $s_n(0) = 1$, we then find

$$\eta(\xi_1^*(\tau))\tfrac{\mathrm{d}}{\mathrm{d}\tau}\xi_1^*(\tau) \ge \tfrac{\mathrm{d}}{\mathrm{d}\tau}\xi_1^*(\tau),$$

while $s_n \le 1$ and $\frac{\mathrm{d}}{\mathrm{d}\tau}\xi_2^*(\tau) \ge 0$ imply

$$-\eta(\xi_2^*(\tau))\tfrac{\mathrm{d}}{\mathrm{d}\tau}\xi_2^*(\tau) \ge -\tfrac{\mathrm{d}}{\mathrm{d}\tau}\xi_2^*(\tau).$$

Hence, we obtain the Hilpert estimate

$$\eta(\xi_1^*(\tau))\tfrac{\mathrm{d}}{\mathrm{d}\tau}\xi_1^*(\tau) - \eta(\xi_2^*(\tau))\tfrac{\mathrm{d}}{\mathrm{d}\tau}\xi_2^*(\tau) \ge \tfrac{\mathrm{d}}{\mathrm{d}\tau}\xi_1^*(\tau) - \tfrac{\mathrm{d}}{\mathrm{d}\tau}\xi_2^*(\tau),$$

and as moreover the right hand side of (3.17) is nonpositive, we infer

$$\big\langle \partial_\tau \overline{P}(\tau,\cdot), s_n(\overline{P}(\tau,\cdot))\big\rangle + 2\left(\tfrac{\mathrm{d}}{\mathrm{d}\tau}\xi_1^*(\tau) - \tfrac{\mathrm{d}}{\mathrm{d}\tau}\xi_2^*(\tau)\right) \le 0. \tag{3.19}$$

Using

$$\big\langle \partial_\tau \overline{P}(\tau,\cdot), s_n(\overline{P}(\tau,\cdot))\big\rangle = \frac{\mathrm{d}}{\mathrm{d}\tau}\int_{\mathbb{R}} S_n(\overline{P}(\tau,\xi))\,\mathrm{d}\xi,$$

where $S_n'(z) = s_n(z)$ and $S_n(0) = 0$, we next integrate (3.19) from τ_1 to τ_2 and arrive at

$$\int_{\mathbb{R}} S_n(\overline{P}(\tau_2,\xi))\,\mathrm{d}\xi + 2\,|\xi_1^*(\tau_2) - \xi_2^*(\tau_2)| \le \int_{\mathbb{R}} S_n(\overline{P}(\tau_1,\xi))\,\mathrm{d}\xi + 2\,|\xi_1^*(\tau_1) - \xi_2^*(\tau_1)|.$$

By construction, $S_n(\overline{P}(\tau,\cdot))$ converges to $|\overline{P}(\tau,\cdot)|$ in $\mathsf{L}^1(\mathbb{R})$ as $n\to\infty$, and passing to the limit yields the desired inequality

$$\|\overline{P}(\tau_2,\cdot)\|_{\mathsf{L}^1(\mathbb{R})} + 2\,|\xi_1^*(\tau_2) - \xi_2^*(\tau_2)| \le \|\overline{P}(\tau_1,\cdot)\|_{\mathsf{L}^1(\mathbb{R})} + 2\,|\xi_1^*(\tau_1) - \xi_2^*(\tau_1)| \tag{3.20}$$

in the case of $\xi_1^* \ge \xi_2^*$ in $[\tau_1,\tau_2]$. Moreover, for $\xi_1^* \le \xi_2^*$ in $[\tau_1,\tau_2]$ we derive (3.20) by repeating the above arguments with $s_n(z) = \max(-1, \min(1, -1+nz))$ for $|z| \le n$, which satisfies $s_n(0) = -1$. Combining both cases and continuity of $\|\overline{P}(\tau,\cdot)\|_{\mathsf{L}^1(\mathbb{R})}$ we finally obtain

$$\|\overline{P}\|_{\mathsf{L}^\infty(I;\mathsf{L}^1(\mathbb{R}))} + 2\|\xi_1^* - \xi_2^*\|_{\mathsf{L}^\infty(I)} \le \|\overline{P}(0,\cdot)\|_{L^1(\mathbb{R})} + 2\,|\xi_1^*(0) - \xi_2^*(0)|\,,$$

so uniqueness follows from $\overline{P}(0,\cdot) = 0$ and $\xi_1^*(0) = \xi_2^*(0)$. □

As a consequence of Theorems 3.16 and 3.18 we obtain the following approximation result.

Corollary 3.19 (uniqueness and improved convergence)**.** *If $P_\varepsilon(0,\cdot) \to P(0,\cdot)$ in $\mathsf{L}^\infty(\mathbb{R})$ as $\varepsilon\to 0$, the limit (P,Q,R,ξ^*) in Theorem 3.16 is unique and the convergence* (3.11)–(3.12) *holds along the whole family $\varepsilon\to 0$.*

A The discrete heat kernel

Denoting by $\widehat{\ }$ the Fourier transform with respect to the discrete spatial variable j, that is

$$\widehat{g}(t,k) = \sum_{j\in\mathbb{Z}} g_j(t) e^{-\imath kj}, \qquad k\in[-\pi,\pi),$$

the initial value problem (3.4) for the discrete heat kernel transforms into

$$\partial_t \widehat{g}(t,k) = \rho(k)\widehat{g}(t,k), \qquad \widehat{g}(0,k) = 1, \tag{A.1}$$

where ρ is the Fourier symbol of the negative discrete Laplacian, i. e.

$$\rho(k) = 2 - e^{-\imath k} - e^{+\imath k} = 2(1-\cos k).$$

Solving the parametrized ODE (A.1) and applying the inverse Fourier transform we find

$$g_j(t) = \frac{1}{2\pi}\int_{-\pi}^{+\pi} \widehat{g}(t,k) e^{\imath kj}\,\mathrm{d}k = \frac{1}{2\pi}\int_{-\pi}^{+\pi} \exp\left(-\rho(k)t\right)\cos\left(jk\right)\mathrm{d}k. \tag{A.2}$$

Lemma A.1 (monotonicity and convexity properties for $j=0$)**.**

1. *$t\mapsto g_0(t)$ is strictly positive, strictly decreasing, and strictly convex.*
2. *$t\mapsto \int_0^t g_0(s)\,\mathrm{d}s$ is strictly positive, strictly increasing, and strictly concave.*

3. $t \mapsto \dot{g}_0(t)$ is strictly negative, strictly increasing, and strictly concave.

Proof. The representation formula (A.2) implies

$$g_0(t) > 0, \qquad \dot{g}_0(t) < 0, \qquad \ddot{g}_0(t) > 0, \qquad \dddot{g}_0(t) < 0$$

for all $t \geq 0$, so all assertions follow immediately. □

Employing standard methods from asymptotic analysis one finds

$$t^{1/2} g_j(t) \quad \xrightarrow{t\to\infty} \quad \frac{1}{2\sqrt{\pi}}, \qquad t^{3/2} \dot{g}_j(t) \quad \xrightarrow{t\to\infty} \quad -\frac{1}{4\sqrt{\pi}}$$

as well as asymptotic laws for the long-time behavior of any discrete moment. For our considerations in §3, however, the following rather rough estimates are sufficient.

Lemma A.2 (temporal decay properties)**.** *There exist positive constants c and C such that*

$$0 \leq g_j(t) \leq g_0(t) \leq C(1+t)^{-1/2}, \tag{A.3}$$

$$|\,\Delta\, g_j(t)| = |\dot{g}_j(t)| \leq -\dot{g}_0(t) \leq C(1+t)^{-3/2} \tag{A.4}$$

and

$$g_0(t) \geq c(1+t)^{-1/2} \tag{A.5}$$

hold for all $j \in \mathbb{Z}$ and all $t \geq 0$. Moreover, we have

$$\sum_{j\in\mathbb{Z}} g_j(t) = 1, \qquad \sum_{j\in\mathbb{Z}} \big|\nabla_+ g_j(t)\big|^2 \leq C(1+t)^{-3/2} \tag{A.6}$$

for all $t \geq 0$ and some constant C.

Proof. For $t \geq 1$ we observe that

$$\frac{1}{4}k^2 \leq \frac{4}{\pi^2}k^2 \leq \rho(k) \leq k^2 \qquad \text{for all} \quad k \in [-\pi, \pi],$$

and this implies

$$|g_j(t)| \leq g_0(t) \leq \frac{1}{2\pi}\int_{-\pi}^{+\pi} \exp\big(-k^2 t/4\big)\,\mathrm{d}k \leq \frac{1}{\pi\sqrt{t}}\int_{-\infty}^{+\infty} \exp\big(-k^2\big)\,\mathrm{d}k = \frac{\sqrt{\pi}}{\sqrt{t}}$$

as well as

$$g_0(t) \geq \frac{1}{2\pi}\int_{-\pi}^{+\pi} \exp\big(-k^2 t\big)\,\mathrm{d}k = \frac{1}{2\pi\sqrt{t}}\int_{-\pi\sqrt{t}}^{+\pi\sqrt{t}} \exp\big(-k^2\big)\,\mathrm{d}k \geq \frac{1}{2\pi\sqrt{t}}\int_{-\pi}^{+\pi} \exp\big(-k^2\big)\,\mathrm{d}k.$$

Combining these estimates with $0 < g_0(1) \leq g_0(t) \leq g_0(0) = 1$ for $0 \leq t \leq 1$ we readily obtain (A.3) and (A.4). Moreover, for $t \geq 1$ we estimate

$$|\,\Delta\, g_j(t)| = |\dot{g}_j(t)| \leq \frac{1}{2\pi}\int_{-\pi}^{+\pi} \rho(k)\exp\big(-\rho(k)t\big)\,\mathrm{d}k = -\dot{g}_0(t) \leq \frac{1}{2\pi}\int_{-\pi}^{+\pi} k^2 \exp\big(-k^2 t/4\big)\,\mathrm{d}k \leq \frac{2\sqrt{\pi}}{t^{3/2}}$$

and this provides (A.5) due to $0 < -\dot{g}_0(t) \leq -\dot{g}_0(0) = -\,\Delta\, g_0(0) = 2$ for all t. The discrete heat equation (3.4) further ensures conservation of mass via $\sum_{j\in\mathbb{Z}} g_j(t) = \sum_{j\in\mathbb{Z}} g_j(0) = 1$. In particular, using discrete integration by parts as well as Hölder's inequality for series we find

$$\sum_{j\in\mathbb{Z}} \big(\nabla_+ g_j(t)\big)^2 = -\sum_{j\in\mathbb{Z}} g_j(t)\Delta\, g_j(t) \leq \|\Delta\, g(t)\|_\infty$$

which implies the estimate in (A.6) thanks to (A.4). □

A further key ingredient to our convergence proof in §3 are the following time-dependent Hölder estimates for $g_j(t)$.

Lemma A.3 (longtime behavior of spatial and temporal Hölder constants)**.** *For each $\gamma \in [0,1]$ there exists a constant C_γ such that*

$$\sup_{t_2 \geq t_1} \frac{\big|g_j(t_2) - g_j(t_1)\big|}{|t_2 - t_1|^\gamma} \leq C_\gamma (1+t_1)^{-\gamma - 1/2}$$

holds for all $j \in \mathbb{Z}$ and all $t_1 > 0$. Moreover, there exists a constant C such that

$$\sup_{j_1, j_2 \in \mathbb{Z}} \frac{\big|g_{j_2}(t) - g_{j_1}(t)\big|}{|j_2 - j_1|^{1/2}} \leq C(1+t)^{-3/4}$$

holds for all $t > 0$.

Proof. Let $j \in \mathbb{Z}$ and $0 < t_1 < t_2$ be fixed. Thanks to (A.4) we estimate

$$\big|g_j(t_2) - g_j(t_1)\big| \leq \int_{t_1}^{t_2} \big|\dot g_j(t)\big| \,\mathrm{d}t \leq C \int_{t_1}^{t_2} (1+t)^{-3/2} \,\mathrm{d}t = C\big|(1+t_1)^{-1/2} - (1+t_2)^{-1/2}\big|,$$

and writing $1 + t_2 = s(1+t_1)$ with $s \geq 1$ we get

$$\frac{|g_j(t_2) - g_j(t_1)|}{|t_2 - t_1|^\gamma} \leq \frac{C f_\gamma(s)}{(1+t_1)^{\gamma+1/2}}, \qquad f_\gamma(s) := \frac{1}{s^{1/2}} \frac{s^{1/2} - 1}{(s-1)^\gamma}.$$

We readily check that the function f_γ is bounded on $[1, \infty)$, so the first claim follows by taking the supremum over $s \geq 1$.

Now let $t > 0$ and $j_1, j_2 \in \mathbb{Z}$ with $j_2 > j_1$ be arbitrary. By Hölder's inequality for series we then find

$$\begin{aligned} \big|g_{j_2}(t) - g_{j_1}(t)\big|^2 &= \left(\sum_{j=j_1}^{j_2-1} \big|\nabla_+ g_j(t)\big|\right)^2 \leq \left(\sum_{j=j_1}^{j_2-1} |\nabla_+ g_j(t)|^2\right)\left(\sum_{j=j_1}^{j_2-1} 1\right) \\ &\leq \left(\sum_{j \in \mathbb{Z}} |\nabla_+ g_j(t)|^2\right)\big(j_2 - j_1\big), \end{aligned}$$

and the second assertion follows from (A.6). □

Acknowledgments

The authors thank Wolfgang Dreyer for pointing them to the problem discussed in the paper. Part of the work has been done at the Harcourt Arms, Cranham Terrace, Jericho, whose hospitality is gratefully acknowledged.

References

[ABF91] N. Alikakos, P. W. Bates, and G. Fusco. Slow motion for the Cahn-Hilliard equation in one space dimension. *J. Differential Equations*, 90(1):81–135, 1991.

[BBMN12] G. Bellettini, L. Bertini, M. Mariani, and M. Novaga. Convergence of the One-Dimensional Cahn–Hilliard Equation. *SIAM J. Math. Anal.*, 44(5):3458–3480, 2012.

[BGN13] G. Bellettini, C. Geldhauser, and M. Novaga. Convergence of a semidiscrete scheme for a forward-backward parabolic equation. *Adv. Differential Equations*, 18(5/6):495–522, 2013.

[BH92] L. Bronsard and D. Hilhorst. On the slow dynamics for the Cahn-Hilliard equation in one space dimension. *Proc. Roy. Soc. London Ser. A*, 439(1907):669–682, 1992.

[BNP06] G. Bellettini, M. Novaga, and E. Paolini. Global solutions to the gradient flow equation of a nonconvex functional. *SIAM J. Math. Anal.*, 37(5):1657–1687, 2006.

[BS96] M. Brokate and J. Sprekels. *Hysteresis and phase transitions*, volume 121 of *Applied Mathematical Sciences*. Springer-Verlag, New York, 1996.

[EG09] S. Esedoḡlu and J. B. Greer. Upper bounds on the coarsening rate of discrete, ill-posed nonlinear diffusion equations. *Comm. Pure Appl. Math.*, 62(1):57–81, 2009.

[Ell85] C. M. Elliott. The Stefan problem with a nonmonotone constitutive relation. *IMA J. Appl. Math.*, 35(2):257–264, 1985. Special issue: IMA conference on crystal growth (Oxford, 1985).

[EP04] L. C. Evans and M. Portilheiro. Irreversibility and hysteresis for a forward-backward diffusion equation. *Math. Models Methods Appl. Sci.*, 14(11):1599–1620, 2004.

[Eva98] L. C. Evans. *Partial differential equations*, volume 19 of *Graduate Studies in Mathematics*. American Mathematical Society, Providence, RI, 1998.

[GN11] C. Geldhauser and M. Novaga. A semidiscrete scheme for a one-dimensional Cahn-Hilliard equation. *Interfaces Free Bound.*, 13(3):327–339, 2011.

[Hil89] M. Hilpert. On uniqueness for evolution problems with hysteresis. In *Mathematical models for phase change problems (Óbidos, 1988)*, volume 88 of *Internat. Ser. Numer. Math.*, pages 377–388. Birkhäuser, Basel, 1989.

[HPO04] D. Horstmann, K. J. Painter, and H. G. Othmer. Aggregation under local reinforcement: from lattice to continuum. *European J. Appl. Math.*, 15(5):546–576, 2004.

[MTT09] C. Mascia, A. Terracina, and A. Tesei. Two-phase entropy solutions of a forward-backward parabolic equation. *Arch. Ration. Mech. Anal.*, 194(3):887–925, 2009.

[NCP91] A. Novick-Cohen and R. L. Pego. Stable patterns in a viscous diffusion equation. *Trans. Amer. Math. Soc.*, 324(1):331–351, 1991.

[Plo94] P. I. Plotnikov. Passing to the limit with respect to viscosity in an equation with variable parabolicity direction. *Differential Eqns.*, 30(4):614–622, 1994.

[PM90] P. Perona and J. Malik. Scale-space and edge-detection using anisotropic diffusion. *IEEE Trans. Pattern Anal. Machine Intell.*, 12(7):629–639, 1990.

[Vis94] A. Visintin. *Differential models of hysteresis*, volume 111 of *Applied Mathematical Sciences*. Springer-Verlag, Berlin, 1994.

[Vis06] A. Visintin. Quasilinear parabolic P.D.E.s with discontinuous hysteresis. *Ann. Mat. Pura Appl.*, 185(4):487–519, 2006.